POWDER METALLURGY OF HIGH DENSITY W-Ni-Cu ALLOYS

A THESIS SUBMITTED TO
THE GRADUATE SCHOOL OF NATURAL AND APPLIED SCIENCES
OF
MIDDLE EAST TECHNICAL UNIVERSITY

BY

NECMETTİN KAAN ÇALIŞKAN

IN PARTIAL FULFILLMENT OF THE REQUIREMENTS
FOR
THE DEGREE OF MASTER OF SCIENCE
IN
METALLURGICAL AND MATERIALS ENGINEERING

SEPTEMBER 2006

Approval of the Graduate School of Natural and Applied Sciences.

Prof. Dr. Canan ÖZGEN
Director

I certify that this thesis satisfies all the requirements as a thesis for the degree of Master of Science.

Prof. Dr. Tayfur ÖZTÜRK
Head of Department

This is to certify that we have read this thesis and that in our opinion it is fully adequate, in scope and quality, as a thesis for the degree of Master of Science.

Prof. Dr. Şakir BOR	Prof. Dr. Bilgehan ÖGEL
Supervisor	Co-Supervisor

Examining Committee Members

Assoc. Prof. Dr. Cemil Hakan GÜR	(METU, METE)	———————
Prof. Dr. Şakir BOR	(METU, METE)	———————
Assoc. Prof. Dr. Kadri AYDINOL	(METU, METE)	———————
Assist. Prof. Dr.Caner DURUCAN	(METU, METE)	———————
Assist. Prof. Dr. Kazım TUR	(ÇU, IE)	———————

I hereby declare that all information in this document has been obtained and presented in accordance with academic rules and ethical conduct. I also declare that, as required by these rules and conduct, I have fully cited and referenced all material and results that are not original to this work.

Name, Last name: Necmettin Kaan ÇALIŞKAN

Signature :

ABSTRACT

POWDER METALLURGY OF HIGH DENSITY W-Ni-Cu ALLOYS

ÇALIŞKAN, Necmettin Kaan
M.S., Department of Metallurgical and Materials Engineering
Supervisor: Prof. Dr. Şakir BOR
Co-Supervisor: Prof. Dr. Bilgehan ÖGEL

September 2006, 90 pages

In the present study; the effects of the powder metallurgical parameters such as the mixing method, compaction pressure, initial tungsten (W) particle size, composition, sintering temperature and sintering time on the sintering behavior of selected high density W-Ni-Cu alloys were investigated. The alloys were produced through conventional powder metallurgy route of mixing, cold compaction and sintering. The total solute (Ni-Cu) content in the produced alloys was kept constant at 10 wt%, while the copper concentration of the solutes was varied from 2.5 wt% to 10 wt%. Mainly liquid phase sintering method was applied in the production of the alloys. The results of the study were based on the density measurements, microstructural characterizations including optical and scanning electron microscopy and mechanical characterizations including hardness measurements.

The results showed that the nature of the mixing method applied in the preparation of the powder mixtures has a considerable effect on the final sintered state of W-Ni-Cu alloys. Within the experimental limits of the study, the compaction

pressure and initial W particle size did not seem to affect the densification behavior. It was found that the sintering behavior of W-Ni-Cu alloys investigated in this study was essentially dominated by the Ni content in the alloy and the sintering temperature. A high degree of densification was observed in these alloys with an increase in the Ni content and sintering temperature which was suggested to be due to an increase in the solubility and diffusivity of W in the binder matrix phase with an increase in these parameters, leading to an increase in the overall sintering kinetics.

Based on the results obtained in the present study, a model explaining the kinetics of the diffusional processes governing the densification and coarsening behavior of W-Ni-Cu alloys was proposed.

Key Words: W-Ni-Cu alloys, Powder Metallurgy, Liquid Phase Sintering, Relative Density, Coarsening.

ÖZ

YÜKSEK YOĞUNLUKLU W-Ni-Cu ALAŞIMLARININ TOZ METALURJİSİ

ÇALIŞKAN, Necmettin Kaan
Yüksek Lisans, Metalurji ve Malzeme Mühendisliği Bölümü
Tez Yöneticisi Prof. Dr. Şakir BOR
Ortak Tez Yöneticisi: Prof. Dr. Bilgehan ÖGEL

Eylül 2006, 90 sayfa

Bu çalışmada karıştırma yöntemi, sıkıştırma basıncı, başlangıç toz boyutu, kompozisyon, sinterleme sıcaklığı ve sinterleme zamanı gibi toz metalurji parametrelerinin yüksek yoğunluklu W-Ni-Cu alaşımlarının sinterlenme davranışı üzerindeki etkileri araştırılmıştır. Bu alaşımlar karıştırma, soğuk sıkıştırma ve sinterlemeyi içeren klasik toz metalurjisi yöntemleri ile üretilmişlerdir. Üretilen alaşımlarda toplam Ni-Cu miktarı ağırlıkça %10'da tutulmuş ve bakır miktarı ağırlıkça %2.5 ila %10 arasında değiştirilmiştir. Bu alaşımların üretiminde başlıca sıvı faz sinterleme yöntemi kullanılmıştır. Çalışmanın sonuçları, yoğunluk ölçümlerine, optik ve taramalı elektron mikroskobu görüntülerini içeren mikroyapı karakterizasyon çalışmalarına ve sertlik testlerine dayanılanarak değerlendirilmiştir.

Sonuçlar göstermiştir ki W-Ni-Cu alaşımlarının hazırlanmasında kullanılan karıştırma yönteminin alaşımların sinterlenmiş son halleri üzerinde önemli miktarda etkisi vardır. Çalışmanın deneysel sınırları içerisinde sıkıştırma basıncı ve başlangıç W toz boyutunun yoğunlaşma sürecine etkisi olmadığı görülmüştür. Çalışmada

incelenen W-Ni-Cu alaşımlarının sinterleme davranışlarının asıl olarak alaşımdaki Ni miktarı ve sinterleme sıcaklığı parametreleri tarafından belirlendiği bulunmuştur. Bu parametrelerdeki artışların çalışılan alaşımlarda yüksek bir yoğunlaşma davranışına yol açtığı gözlenmiştir. Bu olgunun bağlayıcı matris fazı içerisindeki W çözünürlüğü ve yayınımının ve sonuç olarak genel sinterleme hızının bu parametrelerdeki artışa bağlı olarak artmasından kaynaklandığı düşünülmektedir.

Çalışmada elde edilen sonuçlara dayanılarak W-Ni-Cu alaşımlarının yoğunlaşma sürecini ve W tanelerinin irileşmelerini difüzyon prosesleri ile açıklayan bir model önerilmiştir.

Anahtar Sözcükler: W-Ni-Cu alaşımları, Toz Metalurjisi, Sıvı Faz Sinterlemesi, Göreceli Yoğunluk, İrileşme

To my family, Hatice, Nazende and Cumali Çalışkan

ACKNOWLEDGEMENTS

I wish to express my deepest gratitude to my thesis supervisors, Prof. Dr. Şakir BOR and Prof. Dr. Bilgehan ÖGEL for their guidance, their helpful suggestions, prompt feedbacks, endless patience, advice, criticism, encouragements and keen insight throughout the research. This dissertation could not have been completed without their support.

I wish to express my gratefulness to Dr. Kaan Pehlivanoğlu for his help, advice, valuable support and encouragement throughout the entire period of my study.

I would also take the opportunity to thank all my colleagues in TÜBİTAK-SAGE, Metallic and Ceramic Materials Division, for their help and invaluable discussing during my study.

Finally, my most sincere thanks go to my parents and my girlfriend, for their consistent love, understanding, support and encouragement. Without them, this dissertation would have been only a dream.

TABLE OF CONTENTS

CHAPTER 1

INTRODUCTION

The quest for a material having a combination of high strength and ductility, high modulus, good corrosion resistance and high density resulted in the development of W-based alloys. High density W-based alloys are a category of W-based materials that typically contain 90 to 98 wt% W. Most commercial W-based alloys are two-phase structures, the principal phase being nearly pure tungsten in association with a binder phase containing the transition metals (Cu, Ni, Fe, Co) plus dissolved tungsten. Properly processed W-based alloys exhibit a combination of high density, high strength, high ductility, good corrosion resistance, high adsorption capability, and reasonably high toughness. This unique combination of properties have made W-based alloys candidate for both defense and civil applications.

Depending upon the binder composition, W-based alloys can be classified into two main groups; W-Ni-Cu based and W-Ni-Fe based alloys. Historically, the first W-based alloy developed was a W-Ni-Cu alloy. Alloys of this ternary system are still occasionally used today, primarily for applications in which ferromagnetic character and electrical properties are minimized.

Several processing methods can be used in the production of W-based alloys such as arc casting, electron beam melting, swaging, hot extrusion, hot explosive consolidation, chemical vapor deposition and powder metallurgy (P/M) techniques. P/M techniques are generally consolidated to produce W-based alloys for military and civil applications. It is possible, either to press components to shape, or to cut and shape materials subsequent to compaction but prior to sintering. This ability to

produce parts very close to the materials size reduces the amount of final machining necessary to produce the finished components.

The aim of this work is to produce W-Ni-Cu based alloys via powder metallurgical techniques starting from elemental W, Ni and Cu powders. In the scope of this work, P/M techniques are developed to produce W-Ni-Cu based alloys having almost full density through conventional powder metallurgical route of mixing, cold compaction and liquid phase sintering. The effects of the mixing method, compaction pressure, initial W particle size, composition, sintering temperature and sintering time on the sintering behavior of these alloys were investigated on the basis of density measurements, optical and scanning electron microscopy and hardness measurements. Based on the results of the study, a model proposed to explain the kinetics of the diffusional processes governing the densification and coarsening behavior of W-Ni-Cu alloys was developed.

In the present study, all W-Ni-Cu alloy compositions are given in wt% unless otherwise stated.

CHAPTER 2

THEORY

2.1 Introduction to Tungsten (W) Based Alloys

Tungsten is an attractive material because of its high density, melting point and modulus of elasticity. However; production and consolidation of pure tungsten is very difficult due to its high melting point and poor workability. These limitations led to the development of two phase alloys. Tungsten based alloys are a category of W-based materials that typically contain 90 to 98 wt% W. Most commercial W-based alloys are two-phase structures, the principal phase being nearly pure tungsten in association with a binder phase containing the transition metals (Cu, Ni, Fe, Co) plus dissolved tungsten. The typical microstructure of such an alloy is shown in Figure 2.1. As a consequence, W-based alloys derive their fundamental properties from those of the principal tungsten phase, which provides for both high density and high elastic stiffness. It is these two properties that give rise to most applications for this family of materials [1]. Depending upon the binder composition, W-based alloys can be classified into two main groups [2].

(a) W-Ni-Fe based alloys: This group is ferromagnetic. The nickel to iron ratio typically ranges from 1:1 to 4:1. The preferred ratio is 7:3, since this composition avoids the formation of intermetallic phases. W-Ni-Fe based alloys exhibit excellent strength-ductility combinations. They can be cold worked to a reduction of 60% without intermediate annealing.

(b) W-Ni-Cu based alloys: Members of this group are non-magnetic and exhibit a higher electrical conductivity. The nickel to copper ratio ranges from 3:2 to 4:1. These alloys exhibit lower strength and ductility than W-Ni-Fe alloys, but show excellent resistance to most of the common corrosive agents; in dilute solutions of HCl, the resistance to attack is up to twice that of 18/8 stainless steel. These alloys remain stable up to 1000 ^{0}C and exhibit high oxidation resistance up to 400 ^{0}C [2].

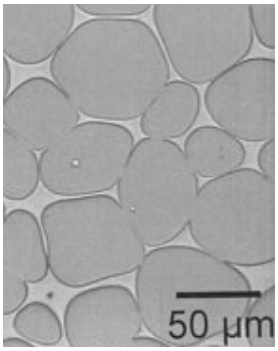

Figure 2.1 The typical microstructure of a W-based alloy, namely, W-7Ni-3Fe alloy produced by liquid phase sintering [1].

The choice of the alloy composition is driven by several considerations. The primary factor is the density required by the given application. Further considerations include corrosion resistance, magnetic character, mechanical properties, and post sinter heat treatment options. Historically, the first W-based alloy developed was a W-Ni-Cu alloy. Alloys of this ternary system are still occasionally used today, primarily for applications in which ferromagnetic character and electrical properties must be minimized [1].

Shortly, the properties make the W-based alloys versatile products as follows [2];

- High density (this unique property makes W-based alloys common material for defeating armor applications)
- High modulus of elasticity
- Excellent vibration damping characteristics
- Good machinability
- High absorption ability for X-rays and γ-rays
- Good thermal and electrical conductivity
- Low electrical erosion and welding tendency
- Good corrosion resistance

The current uses of W-based alloys for civil and military applications can be summarized as below:

- Damping weights for computer disk drive heads
- Balancing weights for ailerons in commercial aircraft, helicopter rotors, and for guided missiles
- Kinetic energy penetrators for defeating heavy armor
- Fragmentation warheads
- Radiation shielding, radioisotope containers, and collimation apertures for cancer therapy devices
- Gyroscope components
- Weight distribution adjustment in sailboats and race cars
- Heavy casings for downbore logging of oil wells
- Weights in premium golf clubs for improving consistency in response
- Low chatter, high stiffness boring bars, and toolholders for metalworking
- Electrical contacts

The unique combination of characteristics that W-based alloys offer for high density applications can easily be seen in Table 2.1.

Table 2.1 Comparison of high-density metals and alloys [1]

Material	Density, g/cm^3	Melting Temperature, °C	Young's modulus, GPa
Iron	7.86	1536	207
Mercury	13.5	-39	Liquid at RT
Tantalum	16.6	2996	186
W-based alloy	17.0-18.5	1450	310-380
Uranium	18.9	1132	160
Tungsten	19.3	3410	410
Gold	19.3	1064	80
Platinum	21.4	1772	147
Iridium	22.5	2443	524

2.2 Fabrication of W-Based Alloys

Several processing methods can be used in the production of W-based alloys such as arc casting, electron beam melting, swaging, hot extrusion, hot explosive consolidation, chemical vapor deposition and powder metallurgy techniques [2]. Since only the production of W-based alloys via conventional powder metallurgy route was investigated in this study, only this technique will be described in detail in the following subsections.

2.2.1 Powder Metallurgy

Powder metallurgy (P/M) is the study of the processing of metal powders that involves fabrication, characterization and conversion of metal powders into useful engineering components. P/M method is one of the most modern methods known for fabrication of metal components. For the last few decades, P/M method is the most promising and emerging field to produce materials with novel properties that cannot be produced by any other technique. The evolution of powder metallurgy industry originated as a means of fabricating refractory metals (W, Nb, Mo, Zr, Ti, and Re) which are quite difficult to fabricate by other techniques because of their high melting points. In fact, tungsten has an historical link with powder metallurgy for many decades.

The P/M processing strategies include application of pressure, deformation and heat to the powders, as a result of which the powders get shaped to a desired component with improved properties. This manufacturing process can be considered to consist of three basic steps; powder mixing, compaction and sintering [2].

2.2.1.1 Powder Mixing (Pre-Compaction Stage)

Examples of operations that take place in the pre-compaction stage include blending, mixing, agglomeration, de-agglomeration and lubrication [3]. Blending and mixing operations are carried out to combine powders into a homogenous mass prior to pressing. Excessive blending may result in significant plastic deformation introducing an undesirable amount of cold work and hence reducing the compressibility. Mixing is usually performed to introduce a lubricant into the powder and to achieve a uniform mixture of the various components. The variables involved in blending or mixing powders include the material, particle sizes, mixer type, mixer size, relative powder volume in the mixer, speed of mixing and time of mixing.

Agglomeration provides a coarser particle size which enables easy flow in automatic forming equipment. Attritioning and deagglomeration are useful in those instances when a fine, discrete powder is needed. Alternatively, fine powders, which do not flow easily due to high interparticle friction, can be agglomerated into coarser particles by any agglomeration techniques. Finally, lubrication of a powder using organic/inorganic agents provides for easier part ejection from compaction tooling and longer die life. It is essential to reduce friction between the pressed compact and the rigid tool components when compacting metal powders in steel or carbide tooling. The lubricants are usually mixed with the metal powder as a final step before pressing. For metal powders, stearates based on, Al, Zn, Li, Mg, or Ca are in common uses. Besides the stearates, other lubricants include waxes and cellulose additives [4].

2.2.1.2 Powder Compaction

Compaction relies on an external source of pressure for deforming the metal powders into a high-density mass while providing shape and dimensional control to the powder. When a metal powder is poured into a die, it will take on a certain packing density. There exist voids exist between the particles, and even with vibration, the highest obtainable density is only the tap density. For a loose powder, there is an excess of void space, no strength and a low coordination number. As pressure is applied to the powder, the first response is a rearrangement of the particles, giving a higher packing coordination. Large pores caused by particle bridging are initially filled by this rearrangement process [3]. Subsequently, the point contacts among the particles begin to deform as the pressure increases. With further increase in the compaction pressure, the amount of plastic deformation that each particle undergoes increases [5]. Plastic flow is localized to particle contacts at low pressures, whereas it occurs homogeneously throughout the compact as the pressure increases. As a result of this, individual particles begin to work harden entirely as the amount of porosity decreases. This work hardening of the particles or the brittleness

of the used materials causes the densification to proceed by fragmentation. Fragmentation causes an increase in the total compact surface area, but the strength of the compact shows little improvement. The extent of these events largely depends on the particle size distribution, particle shape, presence of lubricants, etc. An additional effect of the inter-particle movement is the abrasion of the surface films. These films must be removed before direct metal contact takes place. Some of these films may be rubbed off by particles moving over each other, whereas increasing pressure tends to break-up the films which are usually more brittle than the underlying metal [4].

In the cold compaction of metal powders, different types of pressing techniques such as single and double action hydraulic pressing or cold isostatic pressing (CIP) are used. In the process of single or double action pressing technique, density gradients occur in the compact as a consequence of die wall friction, with the highest density being next to the punch face, as shown schematically in Figure 2.2 Another consequence of powder flowing only in the direction of the applied pressure during compaction is that, when parts with different levels of thickness in the direction of pressing are compacted with only a single punch, they develop different green densities in different levels [1].

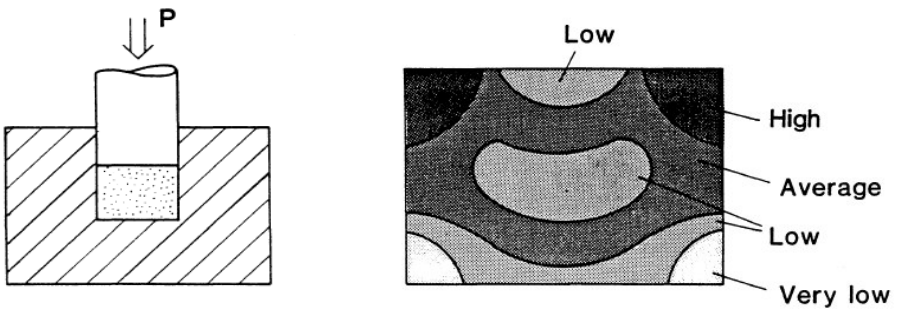

Figure 2.2 Uneven density distribution caused by single end processing in a rigid die [6].

In the process of CIP, a flexible membrane is used to isolate the powder from a liquid medium which is pressurized to cause densification of the powder. Typical mold materials used are made from latex, neoprene, urethane, polyvinyl chloride and other elastomeric compounds. Since the mold moves with the powder as it densifies, friction effects are minimized. Overall compact size and height-to-diameter ratio are limited by the pressure vessel size.

Dimension control in CIP process is generally not as tight as that required in die pressing due to flexible tooling. However, rigid members can be incorporated into the flexible mold assembly to produce accurate surfaces where desired. Ranges of saturation pressures applied in CIP operations are given in Table 2.2, for a variety of powder metals.

Table 2.2 Applicable ranges of saturation pressures applied in CIP for a variety of powder metals [1]

Powder Material	Pressure Range (MPa)
Aluminum	55-140
Copper	140-275
Iron	310-415
High-speed tool steel	240-345
Stainless steel	310-415
Titanium	310-415
Tungsten	240-415
Tungsten carbide	170-205

2.2.1.3 Consolidation or Sintering

Sintering is defined as a thermal treatment for bonding particles into a predominantly coherent solid structure via mass transport events that usually take place at an atomic level. This operation is carried out at temperatures below the melting point of major constituents. The driving force for sintering is the lowering of total surface energy, which occurs by a reduction in total surface area through concomitant formation of inter-particle bonds. Generally, the bonding occurs due to the growth of cohesive necks at the particle contacts [2]. In addition to causing particle bonding, sintering leads to the following important effects: 1) chemical changes, 2) dimensional changes, 3) relief of internal stress, 4) phase changes and 5) alloying. Figure 2.3 summarizes the general sintering processes.

A common characteristic of all forms of sintering is a reduction in surface area with concomitant compact sintering. Most sintering is performed without an

external pressure (pressureless sintering). A major distinction among pressureless sintering techniques is between solid-state and liquid phase processes. Among the solid-state processes, single phase treatments are applicable to pure substances such as nickel, alumina, or copper. On the other hand, mixed phase sintering occurs in an equilibrium two-phase field [3]. The pressure-assisted sintering techniques are newer and represent a hybrid between high-density approaches such as hydrostatic pressing and pressureless sintering.

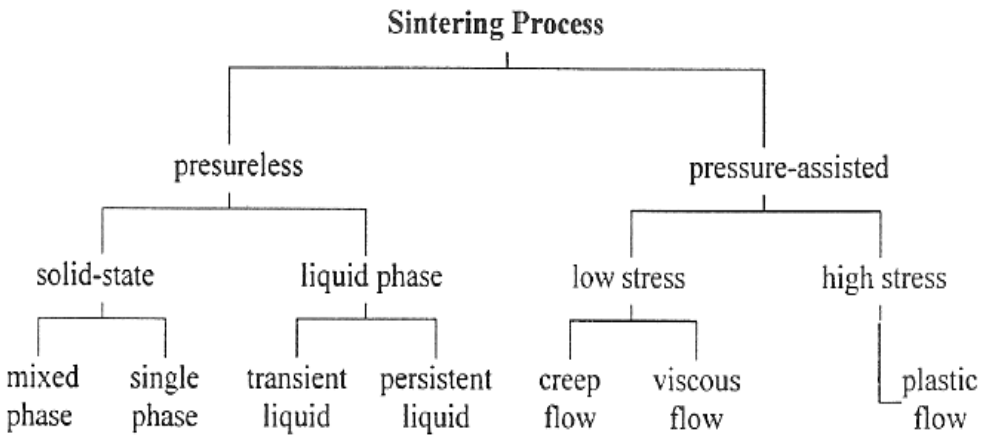

Figure 2.3 Sintering processes and their subdivisions [7].

2.2.1.3.1 Solid State Sintering

Solid state sintering is a process whereby solid bonds form between particles by atomic transport events when the compact is heated. The temperature needed to induce sinter bonding and densification depends on the material and particle size.

Sintering reduces the surface energy by removing free surfaces of the particles, with the secondary elimination of grain boundary area via grain growth. With extended heating, it is possible to reduce the pore volume, leading to compact shrinkage, although in many sintering systems dimensional change is undesirable. Thus, industrial sintering may be focused on densification or on strengthening without necessarily inducing dimensional change [7].

Solid state sintering is proposed to proceed through various stages, schematically shown in Figure 2.4, and through various mass transport mechanisms shown in Figure 2.5

The first stage occurs when particles come into contact, since there is a weak cohesive bond. Initial stage sintering is active for the early portion of neck growth but there is only a minor level of densification. On the other hand, the intermediate stage is the most important stage for densification and determines the properties of the sintered compact. Although there is a considerable neck growth, the actual volume of the neck is small, so it takes a small mass to form a neck.

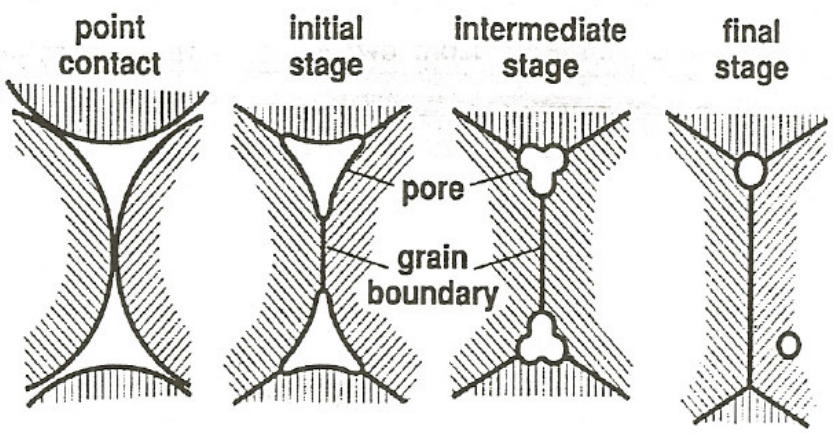

Figure 2.4 Schematic representations of solid state sintering stages [7].

In the intermediate stage, the pore structure becomes smooth, interconnected and approximately cylindrical. The concomitant reduction in curvature and surface area slows down sintering rate with time. It is common for grain growth to occur in the latter portion of the intermediate stage of sintering. An open pore network becomes geometrically unstable when the porosity has shrunk to approximately 8%, because the pores are long in comparison with the shrinking diameter. The somewhat cylindrical pores collapse and pinch off into lenticular or spherical pores. The appearance of these isolated pores indicates the final stage of sintering and slow densification. The driving force is strictly the elimination of the pore-solid interfacial area. Gas in the pores will limit the end point density; accordingly, vacuum sintering can produce high final densities as long as there is no vapor being emitted by the sintering material to fill the pores.

The sintering stages described above contain the path of atomic motion which produces the mass flow. For metal powders, the mass transport mechanisms are primarily surface, grain boundary or bulk diffusion processes, as shown in Figure 2.5.

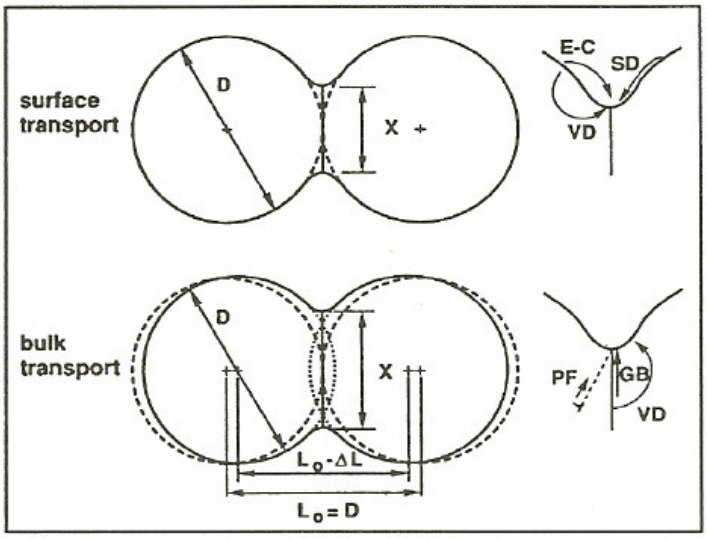

Figure 2.5 Two classes of mass transport mechanisms observed during sintering applied to the two-sphere model (E-C: Evaporation-Condensation, SD: Surface Diffusion, VD: Volume Diffusion, PF: Plastic Flow, GB: Grain Boundary Diffusion) [7].

Surface transport involves neck growth without a change in inter-particle spacing (without densification). It is the result of mass flow originating and terminating at the particle surface and there is no dimensional change. Surface diffusion and evaporation-condensation are the two most important contributors during surface transport controlled sintering. Lattice (volume) diffusion from surface sources to surface sinks is possible but not observed. In contrast to surface transport, bulk transport controlled sintering results in net dimensional changes. The mass originates at the particle interior with deposition at the neck region. The bulk transport mechanisms include volume diffusion, grain boundary diffusion, plastic flow, and viscous flow (for the amorphous solids). Plastic flow is thought to be of minor importance but dislocation motion occurs in the neck region during heating of powders. Therefore, it is considered a transient process, only active during heating.

Although both transport mechanisms result in a loss of compact surface area due to neck growth, the main difference occurs in shrinkage during sintering. Generally, bulk transport processes are more active in the later sintering stages. The importance of these various mechanisms is dependent on the material, particle size, sintering stage, temperature, and several other process variables [7].

2.2.1.3.2 Liquid Phase Sintering

Liquid Phase Sintering (LPS) is a consolidation technique of powder compacts containing more than one component at a temperature above the solidus of the components, and hence in the presence of a liquid. Microstructural changes during LPS are fast because of fast material transport through the liquid. There are two main forms of LPS, persistent LPS and transient LPS. In persistent LPS, the liquid phase persists throughout the high-temperature portion of the sintering cycle and can be formed by use of pre-alloyed powder. In transient LPS, the liquid phase disappears during the sintering cycle, due to dissolution into the solid or formation of a new phase. Only in this case, the liquid alloys with the solid phase which remains solid, and the liquid is present only for a brief period. This process is not used as the primary densification method, but is used to achieve another increment in density. For example, it may be used in high alloy steel or tool steel production to increase the density of a green compact from 80 % to >95 % of full density.

When a liquid phase forms during heating of a powder mixture compact, it flows into the fine capillaries due to the capillary pressure difference between the fine and coarse channels between the solid particles. The solid particles can be redistributed by this liquid flow and in liquid phase sintering models this phenomenon is referred to as particle rearrangement [8]. The possibility of particle rearrangement by liquid flow relies on various factors including not only the liquid volume fraction but also the dihedral angle, the extent of sintering at the moment of liquid formation and particle size. When the dihedral angle is larger than 0^{o},

however, particle rearrangement is expected to be unlikely. After liquid formation, the compact consists of three phases: solid, liquid and vapor. As sintering proceeds, elimination of pores and growth of grains occur simultaneously in a liquid matrix [8].

There are two models and theories that have been developed for explaining densification during liquid phase sintering. One is the classical three-stage model [9] and theory [10] and the other the pore filling theory [11,12,13].

2.2.1.3.2.1 Classical Model for LPS

The classical model and theory of liquid phase sintering proposed that liquid phase sintering can be divided into three stages.1-particles rearangement by liquid flow, 2-contact flattening by a solution/reprecipitation (also called dissolution/precipitation) process, 3-solid state like sintering. Figure 2.6 and Figure 2.7 summarize the stages of classical liquid phase sintering. The processes proposed to occur in these stages are as follows [14];

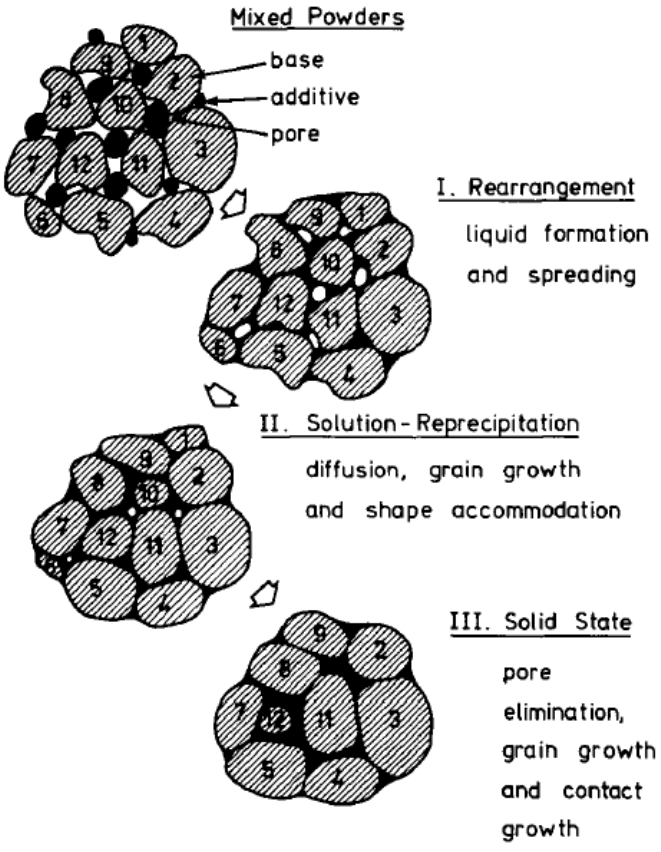

Figure 2.6 The classic stages of LPS involving mixed powders [14].

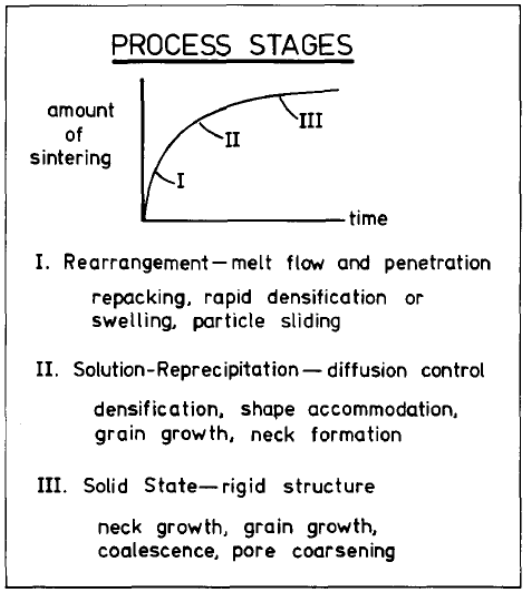

Figure 2.7 The process stages associated with classic LPS [14].

a) Initial Stage: Particle Rearrangement: Initially, the mixed powders are heated to a temperature at which a liquid forms. With liquid formation, rapid densification occurs owing to the capillary force exerted by the liquid. The elimination of porosity occurs as the system minimizes its surface energy. During rearrangement stage, the compact responds as a viscous mass to the capillary action. The elimination of porosity increases the compact viscosity. As a consequence, the densification rate continuously decreases.

The amount of densification attained by rearrangement is dependent on the amount of liquid, the particle size and the solubility of the solid in the liquid. Usually, finer particles give better rearrangement. Full density is possible by rearrangement if enough liquid is formed. Rearrangement can be inhibited by a high green density or irregular particle shape. The particle contacts resulting from

compaction form solid state bonds during heating, thereby preventing rearrangement. Concurrent with the rearrangement stage are various other events, but the kinetics of rearrangement are dominant initially. As densification by rearrangement slows down, solubility and diffusivity effects become dominant. This second stage is termed solution-reprecipitation [14].

b) Intermediate Stage (Contact flattening): The solubility of a grain in its surrounding liquid varies inversely with the grain size; small grains have a higher solubility than coarse grains do. The difference in solubilities establishes a concentration gradient in the liquid. Material is transported from the small grains to the large grains by diffusion, called as Oswald ripening. The net result is a progressively larger grains, giving fewer grains with a wider spacing. In the model, solution-reprecipitation contributes not only to grain coarsening but also to densification [14].

c) Final Stage (Solid state like sintering): Cannon and Lenel [9] suggest that, after considerable densification by a solution/reprecipitation process and the formation of grain boundaries, the contribution of solution/reprecipitation becomes negligible and that the final stage of densification occurs by a sintering process similar to solid state sintering.

2.2.1.3.2.2 Pore Filling Model and Theory

Another model for explaining the densification during LPS was proposed by Kwon and Yoon [11]. Based on microstructural observations during liquid phase sintering, they proposed that filling of pores by the liquid was the essential process for densification and governed the overall sintering kinetics. Later, Park et al [15] theoretically analyzed the liquid filling of isolated pores, and recently, Kang et al [13] developed a new model and theory of liquid phase sintering which describes the densification of LPS in view of the behavior of solid grains without taking the grain

growth into account, and the densification in terms of liquid flow into pores as a result of grain growth. A series of microstructural observations and theoretical analyses suggest that densification occurs essentially by the liquid filling of pores [8].

The pore filling model of LPS was developed via a series of experimental observations involving the examination of microstructural changes during LPS in the W-Ni system and suggested a three stage model, 1-liquid coagulation, 2-liquid redistribution, 3-liquid filling of pores . The pore filling is thought to be a result of grain growth. Figure 2.8 depicts schematically the microstructures at the specimen surface and pore surface during grain growth. Because of the hydrostatic pressure in the liquid, the liquid pressures at the specimen surface and pore surface are the same with the same liquid menisci radius, if the gas pressure in the pore is the same as that outside the specimen. With grain growth, the liquid meniscus radius of the compact increases linearly and can become equal to the pore radius, resulting in complete wetting of the pore surface (the critical moment for the pore filling), as schematically shown in Fig. 2.8 (b). Then, an imbalance of liquid pressures at the specimen surface and pore surface arises with further increase in grain size, because because the liquid meniscus radius at the pore surface is limited by the pore size while that at the specimen surface is not (Fig. 2.8 (c)) [13].

One of the important consequences of the pore filling mechanism is that the pore filling must occur in temporal sequence depending on size: smaller pores earlier and larger ones later. The contributions of pore filling and contact flattening relative to densification can be estimated. The solid volume transported by contact flattening is inconsiderable, while the increase in average grain size is relatively fast. The time needed for densification by pore filling is estimated to be, in general, a few orders of magnitude shorter than that by contact flattening. Furthermore, in this estimation, the contribution of contact flattening is overestimated, because the grain shape is assumed to change during the process from a sphere to one of anhedral equilibrium.

But, from the early stage of liquid- phase sintering, the grain shape is one observably close to anhedral equilibrium for a given liquid pressure in the compact: so the driving force for shape change must be inconsiderable.

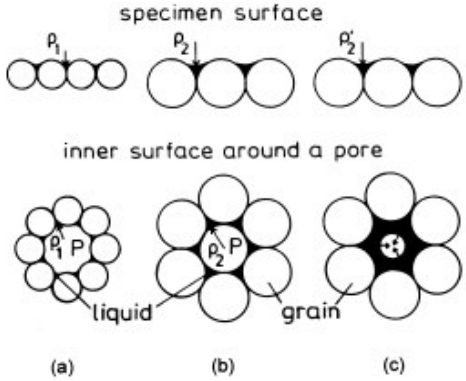

Figure 2.8 Schematic showing the liquid filling of pore during grain growth: (a) before pore filling, (b) critical moment of filling and (c) liquid flow right after critical moment. No effect of gases entrapped in pore is assumed. P is the pore and ρ is the radius of curvature of liquid meniscus ($\rho_1<\rho_2$, $\rho_2\geq\rho_2$`) [13].

Figure 2.9 shows the proposed liquid-phase sintering model. Figure 2.9 (a) depicts schematically the microstructure of a compact containing pores of different sizes. As long as the pores are stable, the volume fraction of liquid surrounding the grains does not change with grain growth. Once the surface of smaller pores is completely wetted as a result of grain growth to the critical size, the liquid spontaneously fills the pores, as illustrated in Fig. 2.9 (b). With the pore filling, the compact density measured by the water-immersion method must increase. In terms of microstructure, however, the result of the pore filling is that the liquid meniscus recede at specimen and intact pore surfaces, and thus there is a sudden decrease in

liquid pressure. The pressure decrease can also be understood as a reduction of the effective liquid volume surrounding the grains in the bulk away from the liquid pockets formed. The situation is similar to the suction of liquid from a dense compact by pores, resulting in a substantially lower fraction of liquid for each grain.

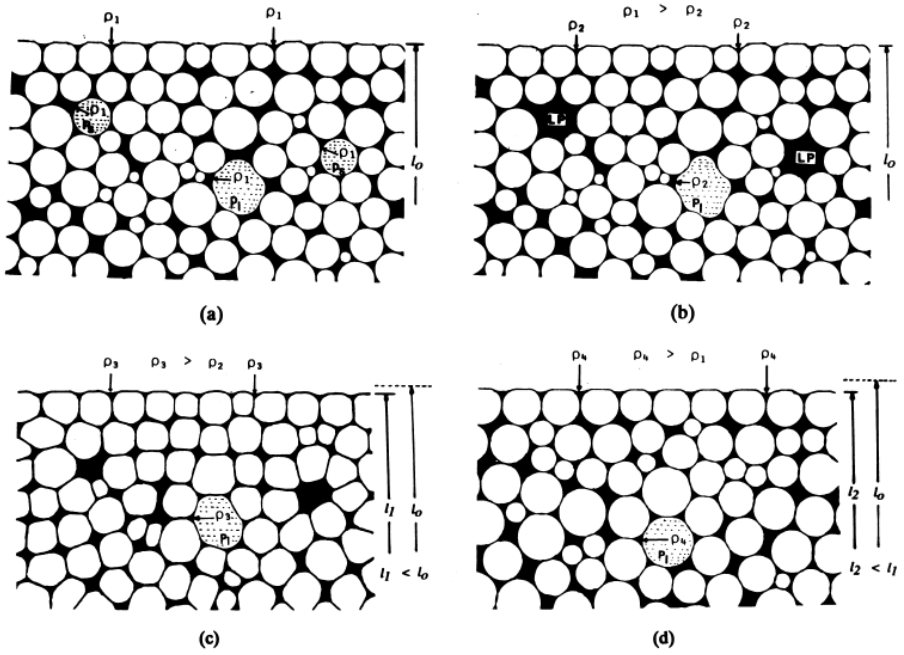

Figure 2.9 Illustrations of pore filling and shape accommodation during liquid-phase sintering: (a) just before liquid filling of small pores (Ps) (at a critical condition), (b) right after filling of small pores, (c) grain shape accommodation by grain growth and homogenization of microstructure around liquid pockets formed at pore sites during prolonged sintering and (d) just before liquid filling of large pore (P_l) [13].

Because of the liquid pressure decrease, i.e. the capillary pressure increase, by pore filling, the shape of the grains tends to become more anhedral during their growth in order to meet the sudden change in liquid pressure. Meanwhile, the homogenization of the microstructure around the liquid pockets formed will proceed, as shown in Fig. 2.9 (c), resulting again in a homogeneous microstructure containing large stable pores. Specimen shrinkage is expected to occur during microstructural homogenization. The microstructural homogenization must contribute to the increase in the effective liquid volume fraction in the bulk except in the liquid pockets. Even though the pore filling model was initially developed for powder compacts containing isolated pores, the pore filling mechanism is believed to be the major densification mechanism from the beginning of liquid-phase sintering. When the particles are rearranged with liquid flow and a skeleton of grains forms, the pores, either interconnected or isolated, are randomly distributed in a dense grain liquid matrix, as typically shown in Figure 2.10 (a) [13].

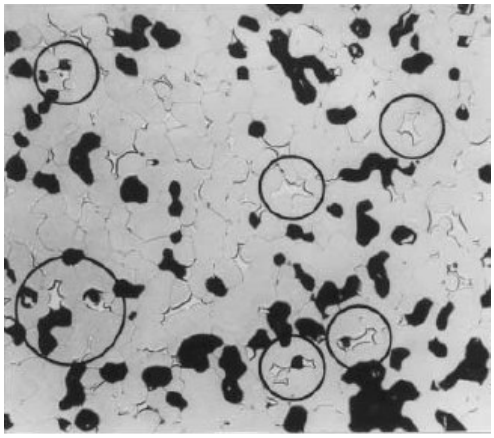

(a)

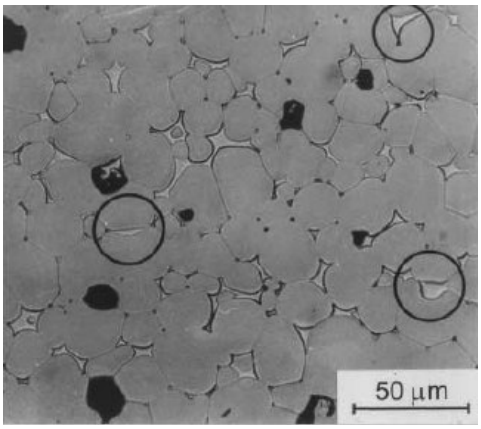

(b)

Figure 2.10 Microstructures of W (5 μm)-1Ni-1Fe specimens sintered at 1460 ^{0}C for (a) 10min and (b) 1h [13].

At this stage, already, some pores are partially or completely filled with liquid as indicated by circles. The shape of the grains in Figure 2.10 (a) does not observably change during extended sintering, as shown in Figure 2.10 (b), implying that a near equilibrium shape for the initial volume fraction of liquid has already been attained at this stage, regardless of the shape and connectivity of the pores.

As explained thus far, the densification kinetics of liquid-phase sintering appears to be controlled by the liquid filling of pores from its beginning, except for the particle rearrangement stage by liquid flow. Therefore, the overall kinetics of liquid-phase sintering is believed to be governed by the pore filling which occurs on the complete wetting of the pore surface by grain growth. The grain growth thus appears to control the pore filling and densification from the beginning of liquid-phase sintering [13]. This theory has been recently proposed, further studies are required to investigate its applicability to other alloy systems.

The fundamental difference between the pore filling model and the contact flattening model is the material transport mechanism for densification. In the former model, the mechanism is liquid flow as a result of grain growth while, in the latter, it is atom-by-atom transport from the contact area to the off-contact area under the capillary pressure of a liquid. As a result, the dependence of densification on grain size in the two models is opposite to each other [8].

2.3 Powder Metallurgy of W-Based Alloys

W-based alloys are W-Ni-Fe or W-Ni-Cu alloys containing 90 to 98% tungsten. Typical nickel: iron ratios range from 1:1 to 4:1, while nickel: copper ratios generally range from 3:2 to 4:1. Minor amounts of other metals can also be added to these alloys. These alloys are generally prepared by LPS and hence can exhibit these alloys achieve essentially full theoretical density. They exhibit good machinability and can have substantial ductility. For example, a 90W-7Ni-3Fe alloy may exhibit an

elongation as high as 40%. Copper-containing alloys are less ductile and are more difficult to sinter to full density, especially in larger cross sections.

W-based alloys are made from blends of elemental powders. Homogeneity is of prime concern, so fine tungsten powders in the 2 to 8 μm range are used. Standard production procedures for tungsten powder yield fine particle sizes. Carbonyl powders are used in iron and nickel blends, and fine electrolytic powder is used in copper blends. As a precaution against impurities and agglomerates, powders are screened to -200 mesh prior to blending. Any standard powder blending procedure can be used [1].

Likewise, almost any P/M compaction procedure can be used in the compaction of powders. If die pressing is used, a binder must be added to the powder. Like pure tungsten powder, high pressed densities cannot be achieved in W-based alloys [16]. (A die-pressed piece typically is about 55% dense, while an isostatically pressed piece is about 65% dense) Consequently, allowance must be made for considerable shrinkage during sintering.

Sintering of W-based alloys can be carried out in any furnace capable of sustaining the temperature and atmosphere required. Generally, the pieces are supported on aluminum oxide sand or aluminum oxide fixtures. Good control of temperature and heating rate is essential to produce consistent, high-quality W-based alloys.

Sintering of high density W-based alloys is mostly done in pure hydrogen atmosphere. Tungsten powder compacts are known to show poor densification during sintering in a non reducing atmosphere, such as Ar or vacuum. This fact is generally attributed to the effect of the oxide film present at the surface of W powder particles, which are thought to impede the sintering and bonding process between W particles [17]. Regardless of the atmosphere used during sintering, a cleanup step in

hydrogen at about 1000 °C is advised [1]. For small pieces, only a few minutes at the mentioned temperature is sufficient; large pieces may require an hour or more.

Although it is possible to solid sinter W-Ni-Fe alloys to near-theoretical density this is not so for W-Ni-Cu alloys because of the low melting point of copper. Therefore, these alloys are prepared through LPS. In the course of LPS, W-based alloys densify as tungsten particles grow by dissolution and subsequent coarsening and coalescence of the tungsten particles. Tungsten particles grow from 3 to 8 μm to rounded grains of 50 to 150 μm in diameter. As the tungsten content of the alloy increases, grain size tends to increase.

In W-Ni-Cu alloys, the low melting point of the copper and the wide liquidus temperature range of the matrix phase make it difficult to achieve full density in large parts. Normally, these alloys are sintered at 1380 °C to 1450 °C. Very low heating rates that begin near the melting point of copper are required to properly sinter these alloys. Sintering times vary from less than an hour for small parts to several hours for large billets. One advantage of these alloys is that they do not have the strong tendency to slump (distort) as W-Ni-Fe alloys do. LPS of W-Ni-Fe alloys is carried out at 1450 °C to 1600 °C, with sintering temperature generally increasing with tungsten content. Heating rates are not as critical as with W-Ni-Cu alloys.

On cooling from liquid-phase temperatures, some problems may be experienced. If small pieces are cooled rapidly from the liquid phase, a solid shell forms around the outer regions of the part, thus causing the liquid matrix to be drawn from the center of the part in an effort to compensate for solidification shrinkage. As a result of this, porosity may subsequently be produced at the center of thicker sections [1].

2.3.1 Production of High Density W-Ni-Cu Alloys by Powder Metallurgy

Studies on W-Ni-Cu alloys have shown that two factors appear to be of relatively more importance in producing alloys with near full density. These factors are the total percentage of Ni-Cu in the alloy composition and the Ni:Cu ratio. It has been shown that the maximum density is obtained when Ni:Cu ratio is about 2 to 1, and the tungsten content is between 89 and 93 percent for an optimum sintering temperature range of 1400-1500 ^{0}C [18]. The optimum value of Ni:Cu ratio appears to result from two opposing effects, which can be best be explained on the basis of an examination of W-Ni-Cu ternary phase diagram. The liquidus projection and 1400 ^{0}C isothermal section of W-Ni-Cu ternary phase diagram are given in Figure 2.11 and Figure 2.12, respectively. As can be seen in Figure 2.11, the liquidus temperatures increase in Ni:Cu ratio. Therefore, W-Ni-Cu alloys with too high Ni:Cu ratio should have to be sintered at relatively high temperature to ensure sintering in the presence of a fully liquid matrix phase, which is an obvious disadvantage.

As a result, lower Ni:Cu ratios are preferable to carry out LPS at lower temperatures. On the other hand, too low Ni:Cu ratios result in a too low W solubility in the liquid phase, as can be seen in Figure 2.11 and Figure 2.12. Since a certain degree of W solubility is required for good sinterability, too low Ni:Cu ratios are also undesirable. Therefore, an optimum Ni:Cu ratio is thought for achieving good sinterability at relatively low temperatures.

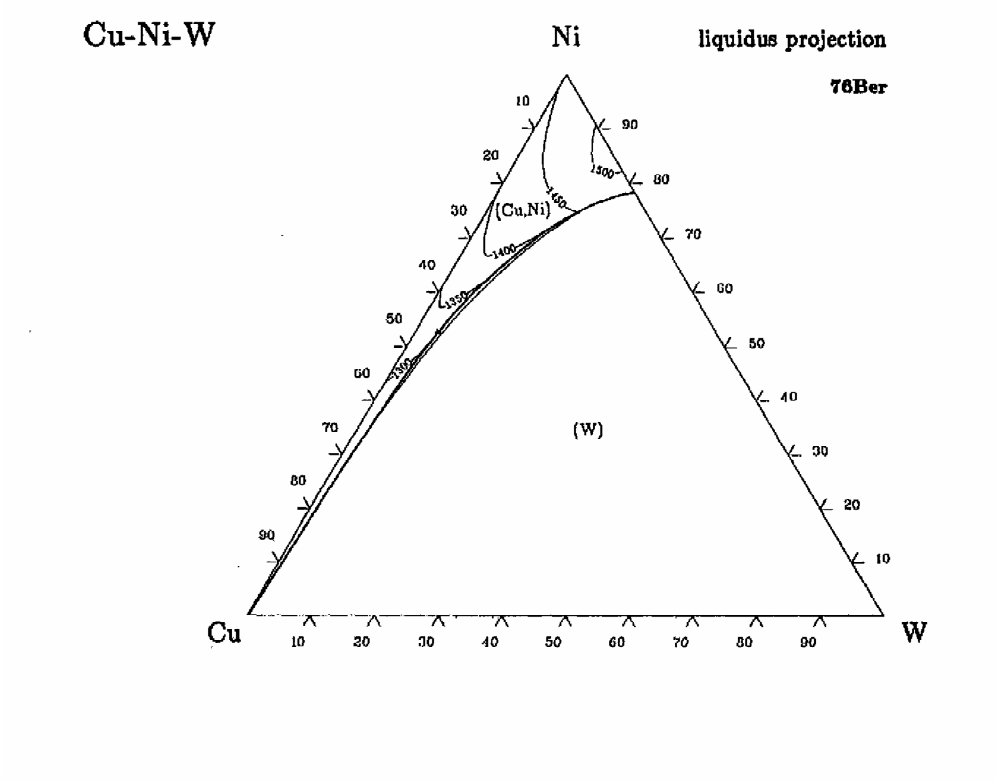

Figure 2.11 Liquidus projection of W-Ni-Cu ternary phase diagram [19].

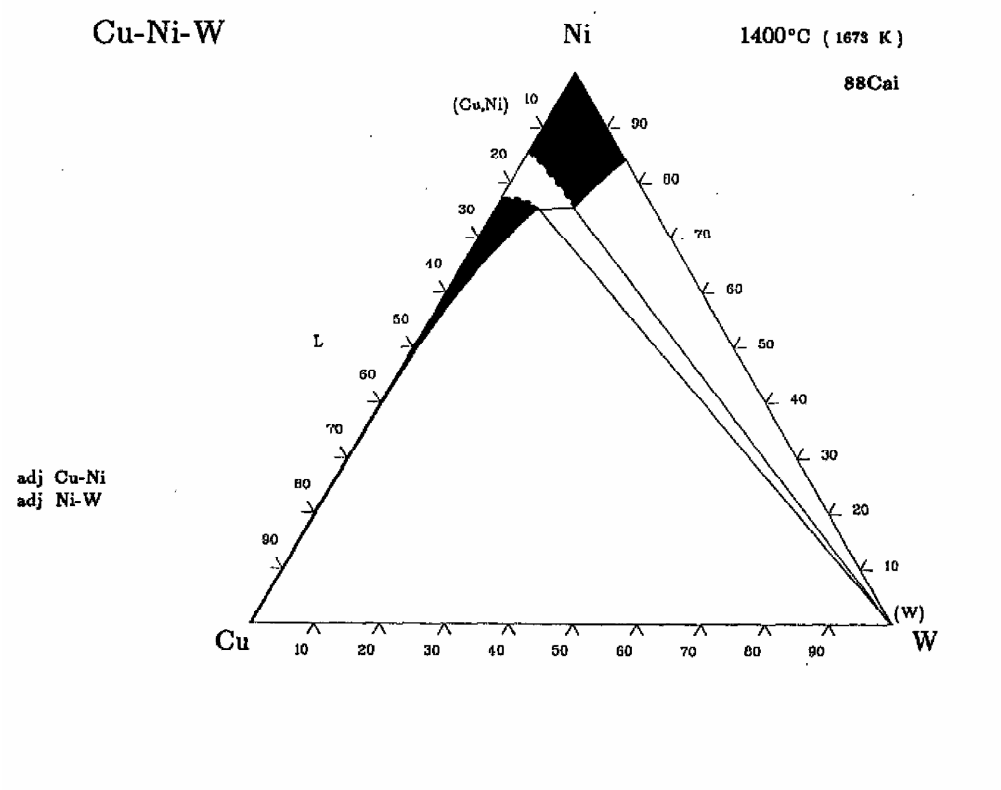

Figure 2.12 Isothermal section of W-Ni-Cu ternary phase diagram at 1400 ^{o}C [19].

The effect of total binder content and sintering temperature on the densification and microstructure of W-Ni-Cu alloys were studied by Ramakrishanan and Upadhyaya [20]. For this purpose, the binder composition in all cases was kept constant at 7:3(Cu:Ni) and the binder content was increased from 5 to 25 wt% in steps of 5 wt%. It was observed that the average grain size of tungsten particles decreases with increase in binder content and increases with increase in sintering period for W(75-95 wt%)-(Cu:Ni ratio of 7/3), as can be seen in Figure 2.13.

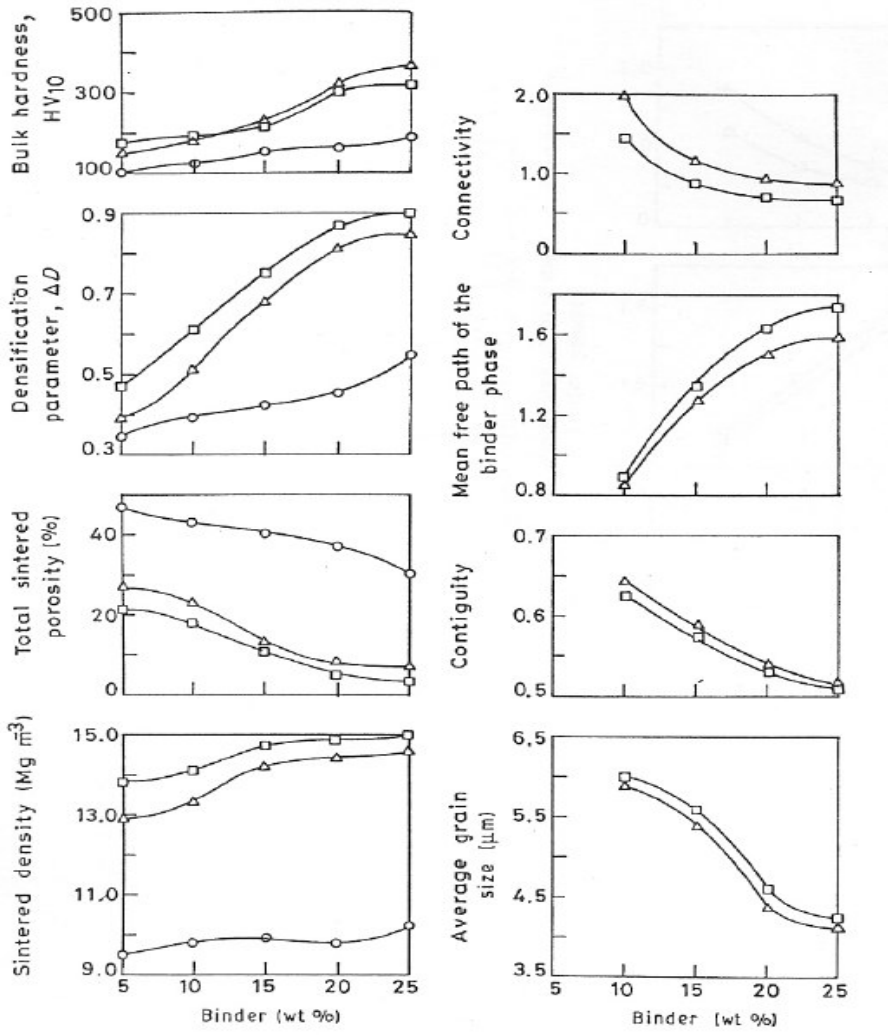

Figure 2.13 Variation of the sintered properties of W (75-95 wt%)-(Cu:Ni ratio of 7/3) alloy compacts with respect to binder content at 1300 ^{0}C (o)0 min, (Δ)60 min, (□)120 min [20]

The effect of the variation of Ni:Cu ratio on the sintering behaviour of W-Ni-Cu alloys having 90 wt% W was studied by Srikanth and Upadhyaya [21]. In their work, it was concluded that with increasing nickel content and sintering temperature enhances densification. They showed that hardness increases appreciably with increasing the nickel amount and sintering temperature (Figure 2.14.).

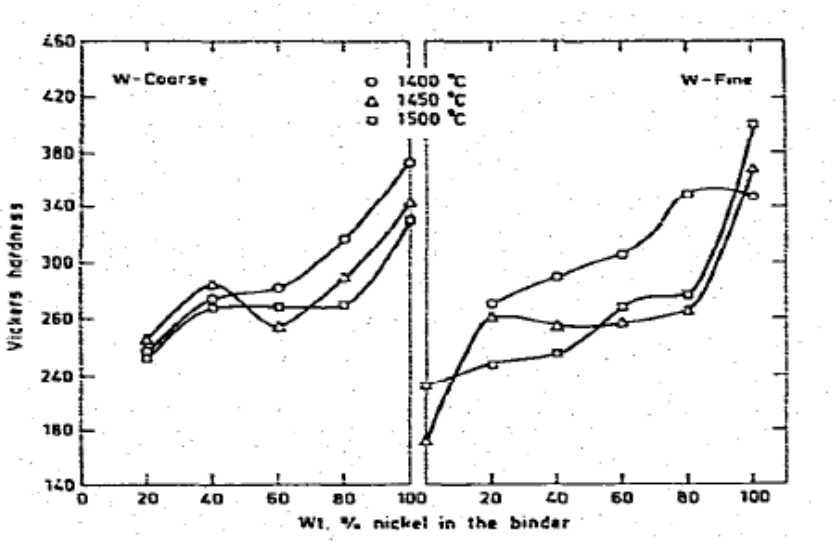

Figure 2.14 Effect of Ni content on the hardness W-Ni-Cu alloys [21]

The effect of sintering temperature and time on the sintered density of W-based alloys were studied by Price, Smithelles and Williams [18]. It was concluded that the liquid formation greatly aids the densification of W-Ni-Cu alloys by increasing the sintering temperature (Figure 2.15) and that the sintered density increases with increasing in sintering time (Figure 2.16)

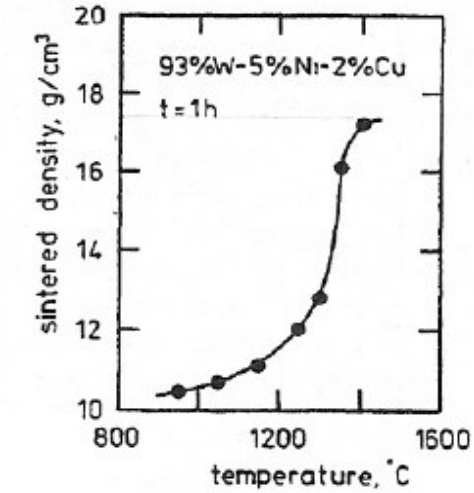

Figure 2.15 Effect of sintering temperature on the sintered density of W-5Ni-2Cu alloys [18].

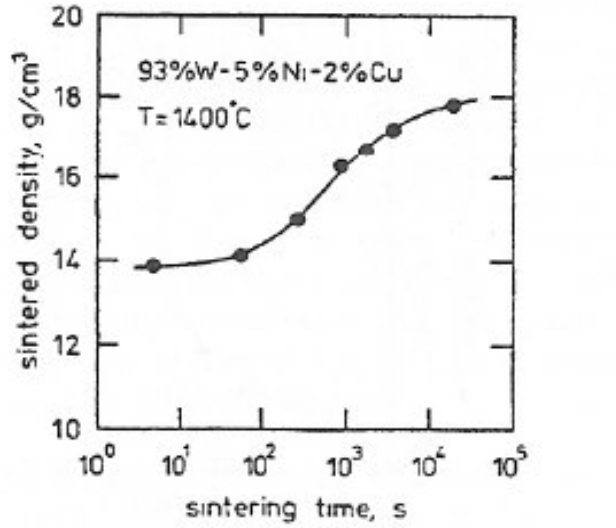

Figure 2.16 Effect of sintering time on the sintered density of W-5Ni-2Cu alloy [18].

Kothari [22] has studied the kinetics of liquid phase sintering of W-Ni-Cu alloys having 11 wt. % constant binder content in the temperature range of 1200-1500 ^{o}C. The sintering operations were carried for different periods of time at each temperature under argon atmosphere. He showed that growth rate of W particles was proportional to $t^{1/3}$ where "t" is the sintering period (Fig 2.17).

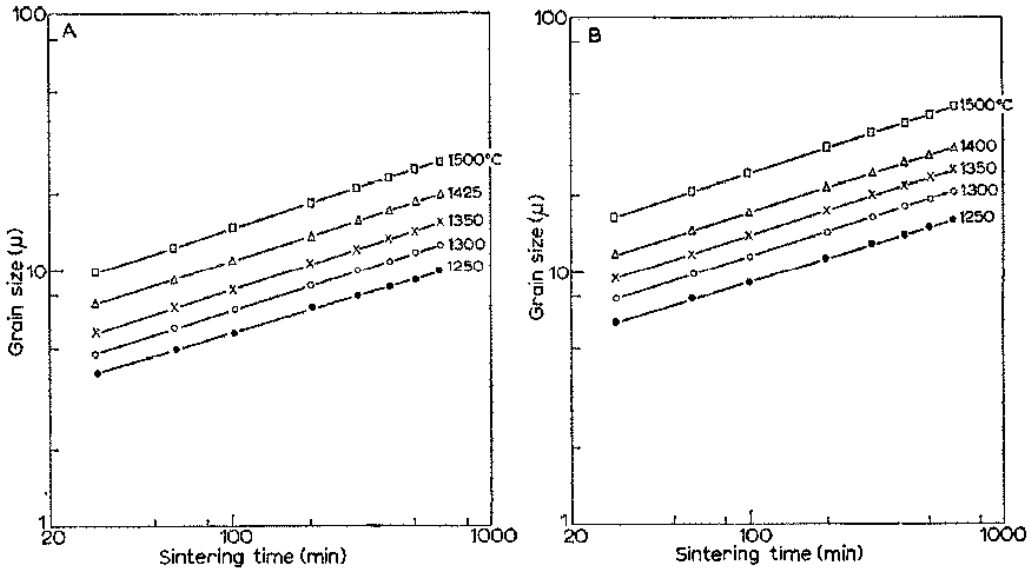

Figure 2.17 Plot of log average grain size with respect to log sintering time (A)89W-3Ni-8Cu alloy (B)89W-7Ni-4Cu [22].

Makarov et al [23] studied the coalescence phenomena in W-Ni-Cu alloys during liquid phase sintering. They found that higher sintering temperature helps in better spherodization at elevated temperature (at 1500^{o}C) sintering.

CHAPTER 3

EXPERIMENTAL PROCEDURE

In the present study, several tungsten based high density W-Ni-Cu alloys were produced through conventional powder metallurgy route of mixing, cold compaction and sintering. The total solute content in the powder mixtures was kept constant at 10 wt%, while the copper composition of the solutes was varied from 2.5 wt% to 10 wt%. The alloys produced were then subjected to microstructural and mechanical characterization through use of relevant techniques. The materials used in the study, the compositions of the W-Ni-Cu based tungsten high density alloys investigated, the experimental procedures applied in alloy preparation and the characterization studies carried out on the produced alloys will be introduced in detail in the following subsections.

3.1. Alloy Preparation

3.1.1 Raw Materials:

Elemental W, Ni and Cu powders with the characteristics given in Table 3.1, namely the average particle size, purity, shape and the source of the powders, were used in the present study. The shape and relative size distribution of elemental powders are presented in Figure 3.1 and Figure 3.2. As can be seen in Table 3.1, the aim of using these different W powders was to investigate the effect of particle size on the sinterability of W-Ni-Cu alloys. Spherical Ni and Cu powders having significantly smaller APS (average particle size) were used to achieve better homogeneity, capillarity and densification in liquid phase sintering [18].

Table 3.1 Characteristics of the W, Cu and Ni elemental powders used in this study

Elemental Powder	APS (μm)	Purity (wt%)	Shape	Source& Sample Code	Concetration Range in the produced alloys (wt%)
W#1	2.5	99.92+	Polygonal	Eurotungstene AW2130	90-100
W#2	6	99.92+	Polygonal	Eurotungstene AW2118	90-100
Cu	3	99.9+	Spherical	AEE Cu-101	0-10
Ni	6	99.9+	Spherical	AEE Ni -110	0-7.5

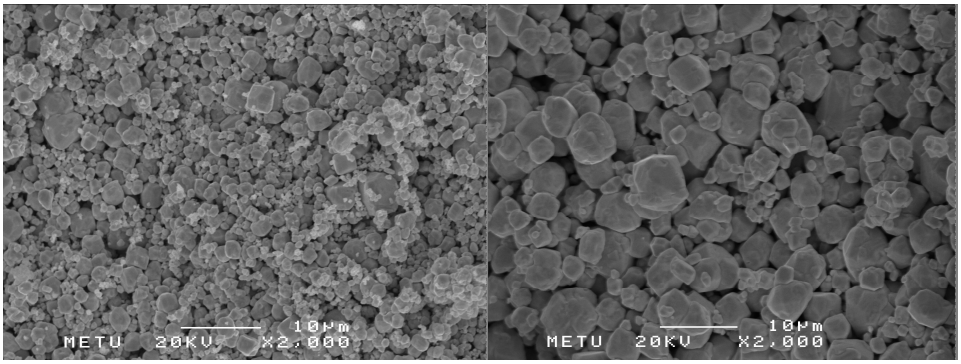

a) W#1 **b) W#2**

Figure 3.1 Shape and relative size distribution of elemental W powders

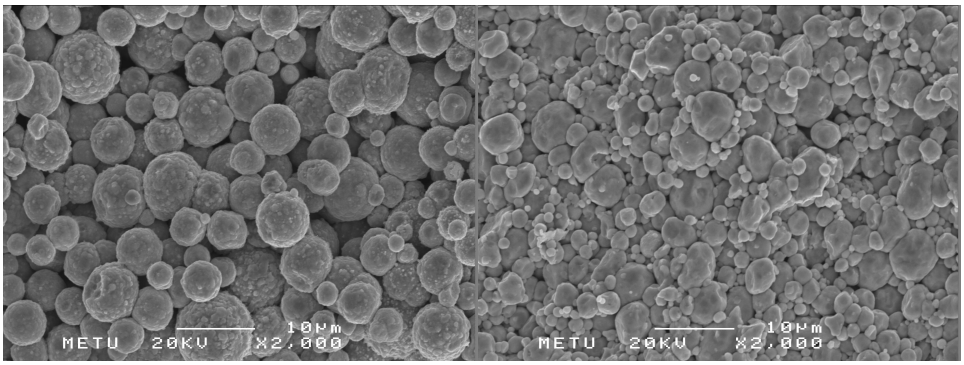

a) Ni **b) Cu**

Figure 3.2 Shape and relative size distribution of elemental Cu and Ni powders

3.1.2 Alloy Systems Investigated

Elemental powders were weighed in a Sartorius CP3200S Model Precision Balance to 0.01 g accuracy to give the alloy compositions given in Table 3.2. The amount of W was kept constant at 90 wt% for all alloys except for the pure W sample. The W powder having 2.5 μm was used only in the preparation of W6-1, as indicated in Table 3.2.

Table 3.2 Nominal compositions of the investigated W-Ni-Cu Alloys

Alloy Number	Ni (wt%)	Cu (wt%)
W0	-	10
W1	1	9
W2	2.5	7.5
W3	3	7
W4	4	6
W5	5	5
W6	6	4
W6-1*	6	4
W7	7	3
W8	7.5	2.5
Pure W	-	-
*Elemental W powder having APS of 2.5 μm was used		

W-Ni-Cu alloy samples were prepared through conventional powder metallurgy route of mixing, cold compaction and sintering, explained in detail in the following subsections.

3.1.3 Mixing Studies of W-Ni-Cu Alloys

To determine the optimum mixing method for achieving uniform powder distribution and hence alloy homogeneity, after sintering, a series of mixing experiments were conducted on a selected W-Ni-Cu alloy, namely W5 alloy. In these experiments, four different mixing methods described below were applied to W5 alloy samples.

1- All elemental powders were put together at once and mixed for an hour.
2- 0.5 wt% Zinc Stearate was added as a lubricant to the powder mixture and the resultant mixture was mixed for an hour.
3- 3 cm^3 Ethanol was added to the powder mixture to reduce the effect of electrostatic charge and resultant mixture was mixed for an hour.
4- Initially, Cu and Ni powders as binders were mixed for an hour, W powder was added later and the resultant mixture was mixed for one more hour.

All mixing experiments were carried out in a Turbula® Shaker Mixer(Model T2F Glenn Mills Inc) at a speed of 67 rpm in a sealed polyamide container (250 cm^3) for 1h. Tungsten carbide balls with a diameter of 4.76 mm were also charged with powders to reduce agglomeration and density gradients. The ball to powder weight ratio was kept at 10:1.

Specimens taken from the W5 alloy mixtures prepared by the above mentioned methods were then preformed by cold compaction at 400 MPa and sintered at 1420^oC under pure Hydrogen atmosphere. According to the comparison based on sintered densities and theoretical densities and evaluation of energy dispersive spectroscopic (EDS) analysis of sintered specimens, the suitable mixing technique was determined, and this technique was then applied in the preparation of other compositions of the W-Ni-Cu alloys given in Table 3.2.

3.1.4 Cold Compaction of W-Ni-Cu Alloys

Two different compaction techniques were applied to produce the W-Ni-Cu alloy green compacts, namely die compaction and cold isostatic pressing (CIP).

3.1.4.1 Die Compaction of W-Ni-Cu Alloys

Disc-shaped specimens with 15 mm diameter and approximately 5 mm height were prepared by a single-acting hydraulic press of 50 tons capacity (Arı Hidrolik AHP-K 150.e) in a hardened SAE/AISI 4140 steel die. Pressing time and velocity were adjusted by the control panel of the press to 30 seconds and 20 mm/s, respectively. The height of the specimens was kept at an optimal minimum to reduce density gradients in the green compact. A Zinc Sterate-Ethanol mixture in a ratio of 100gr/1000cm^3 was used for die wall lubrication prior to powder filling.

3.1.4.2 Cold Isostatic Compaction of W-Ni-Cu Alloys

A cold isostatic press (CIP42260, Flow Autoclave Engineers,) of 414 MPa capacity was used for compacting powder mixtures. Disc-shaped specimens with 15 mm diameter and approximately 5 mm height were prepared by using polyurethane wet bags of Shore A 40 hardness. The bags were fully filled with powder mixtures prior to pressing to reduce the liquid leakage into the bags. The necks of the bags were wrapped and tied securely with banding tapes so that no liquid or air could seep into the bags during pressing. In the pressing operation, the wet bag-powder mixture assembly was put in the CIP, the pressure was raised to the required level and the powder mixture was compressed into the desired form. After the pressing cycle was completed, the entire assembly was removed from the isostatic press, and the green compact was removed from the wet bag for the following sintering operation.

3.1.5 Sintering Studies of W-Ni-Cu Alloys

To determine the optimum sintering parameters for W-Ni-Cu alloys, the effect of sintering temperature and time, compaction pressure and average particle size of tungsten particle size were investigated by using W3, W6, W7 alloys. Sintering temperatures of these alloys were determined according to the binary phase

diagram of Cu-Ni alloys given Figure 3.3. The experiment matrix applied to the alloys is presented in Table 3.3. Since, CIP was used in this study has a capacity of only 414 MPa, the compaction pressures higher than 400 MPa were achieved by single action hydraulic press.

Table 3.3 The experiment matrix applied to W-Ni-Cu alloys

Alloy	Compaction Pressure (MPa) at 1420 ^{0}C for 60 min					Sintering Temperature (^{0}C) for 60 min with 400 MPa			Sintering Time (min) at 1420 ^{0}C with 400 MPa		
	200	300	400	700	1000	1330	1375	1420	15	30	60
W3			√			√	√	√	√	√	√
W6	√	√	√	√	√	√	√	√	√	√	√
W6-1			√	√	√			√			√
W7			√			√	√	√	√	√	√

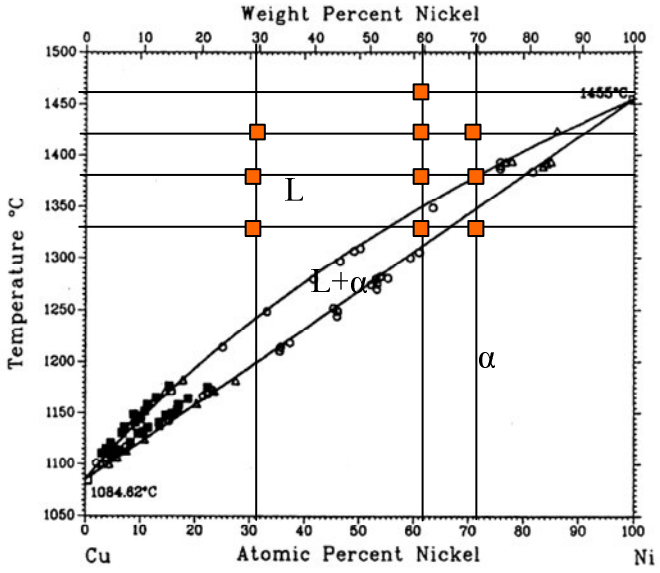

Figure 3.3 Cu-Ni binary phase diagram [24].

The information gathered in these experiments was then applied to other compositions of W-Ni-Cu in which the binder in the powder mixtures was kept constant at 10% by weight, but the Cu content of the Cu-Ni binder was varied from 2.5 wt% to 10 wt% Cu. Rest of the alloys was mixed by using Turbula® shaker, compacted under different pressures in cold isostatic press(CIP); and compacts were heated to 1420^{o}C at a heating rate of 10^{o}C/min and sintered at this temperature for 60 min under pure and dry H_2 atmosphere ($T_{dewpoint} \leq$ -60 ^{0}C). Sintering cycle applied to the alloys was given in Figure 3.4.

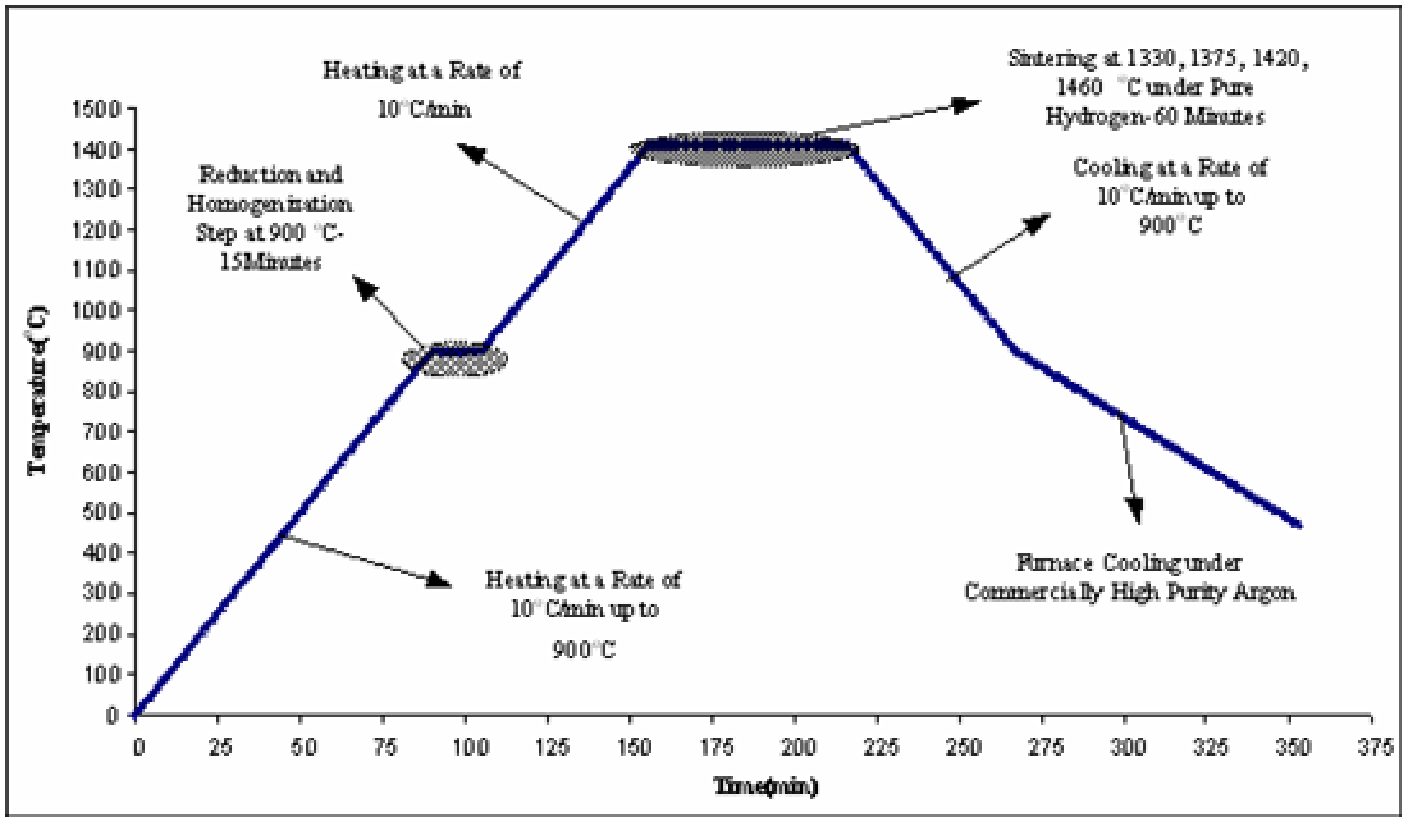

Figure 3.4 General Sintering cycle applied to W-Ni-Cu Alloys.

Sintering experiments were conducted in a molybdenum silicide heated horizantal tube furnace (Protherm PTF 17/75/400). The temperature uniformity of the furnace was $\pm 5\,^{o}C$ along a hot zone of 100 mm. The furnace was controlled by a B-type thermocouple connected to the proportional integrative derivative (PID) type controller; while, one S-type thermocouple was also used to measure the specimen temperature.

The green compacts were sintered under the reducing atmosphere of commercially high purity hydrogen (dew point< -65°C). The flow rate of hydrogen was kept constant at approximately 0.5 l/min. Before feeding hydrogen in to the furnace, furnace chamber was purged with commercially high purity argon to prevent any reaction between pure hydrogen and air. Moisture of hydrogen entering the furnace was continuously controlled by a dew-point meter (KIMO TH 300 wall-type). During cooling; high purity argon at a very low rate of flow was used to prevent oxidation of the sintered compacts.

3.2 Structural Characterization

3.2.1 Microstructural Characterization

3.2.1.1 Sample Preparation

W-Ni-Cu alloys were prepared by conventional metallographic techniques using SiC emery papers from 80 through 2400 grit. Specimens were polished by using 1 μm and 0.05 μm Al_2O_3. Etching was carried out using Murakami's reagent which is composed of 10 g $K_3Fe(CN)_6$ (potassium ferricyanide), 10g KOH or NaOH, 100 ml H_2O.

3.2.1.2 Microstructural Examination

Microstructural examination of the alloy samples was carried out both under an optical microscope and in a scanning electron microscope (SEM).

Zeiss Axioskop 2 Mat optical microscope was used for metalographic examinations. Colored and black-white micrographs were taken using Axio Cam MRc 5 camera connected to the microscope. Scanning electron microscope studies were performed using a Jeol 6400 JSM SEM operated at 20 kV. Both secondary imaging and backscatter imaging modes were applied on all sintered specimens. Northern Tracor Energy Dispersive Spectroscopy (EDS) analysis system attached to the scanning electron microscope was used for the EDS analysis of the specimens.

%Area of binder matrix phase and the average particle size of W particles in the sintered alloys were determined by using a Struers Image analyzer (Scentis Image Analyzer).

3.2.2. Mechanical Characterization

3.2.2.1 Density Measurements

The density measurements of the alloy specimens were carried out on the Basis of Archimedes' principle by using a Sartorius CP224S Precision Balance. The method applied in the measurements is described below;

1. The specimen is first dried until it reaches a constant mass and then cooled to room temperate. The mass of the specimen is then determined in air (m_1).

2. The specimen is then saturated until the open pores are filled with the saturation liquid, namely Xylene with an average density of 0.875gr/cm^3.The apparent mass of the saturated specimen is then determined using a hydrostatic balance. The specimen must be completely immersed in a beaker filled with the saturation fluid for buoyancy (m_2).
3. Then the mass of the saturated specimen is determined by weighing in air (m_3). Xylene that remains on the surface of the specimen must be removed before weighing. The weighing operation should be performed quickly, to avoid loss of mass due to evaporation.
4. Finally, green densities and sintered densities of the samples was then determined by using the equation (1) given below;

$$\rho_b = \frac{m_1}{m_3 - m_2}\rho_l \qquad \textbf{(1)}$$

Where; ρ is the density of the liquid and ρ_b is the density of the sample. These experimentally determined densities were then compared to theoretical densities (ρ_{th}), which were calculated by using equation (2) given below.

$$\frac{1}{\rho_{th}} = \frac{W_{Ni}}{\rho_{Ni}} + \frac{W_{Cu}}{\rho_{Cu}} + \frac{W_W}{\rho_W} \qquad \textbf{(2)}$$

Where W and ρ with the corresponding subscripts denote the weight fraction and bulk density of the elemental powders respectively. Before going on further, it should be emphasized that the equation used in theoretical density determination assumes that there is no reaction or solubility among the constituent alloying elements. Therefore, in cases where these assumptions are not satisfied (such as in the present

study), ρ_{th} values calculated by use of this equation may not represent actual values, and hence these density values should only be treated as a first-order approximation to the actual ones.

3.2.2.2 Hardness Tests

Shimadzu HMV-2 Vicker Hardness Tester at 1kg load was used to measure micro hardness of sintered compacts, respectively. Ten indentations were taken for each sample and the average value was reported.

CHAPTER 4

RESULTS AND DISCUSSION

In this part; the effect of powder metallurgical parameters such as mixing method, compaction pressure, initial W particle size, composition, sintering temperature and sintering time on the sintering behavior of W-Ni-Cu alloys are presented. The result of the studies are based on the density measurements, microstructural characterizations including optical and scanning electron microscopy and mechanical characterizations including hardness measurements described in experimental procedure section.

4.1 Mixing Studies of W-Ni-Cu Alloys:

It was cited in the literature that a high degree of homogeneity in the green microstructure is significantly important for the LPS processes to achieve homogeneous sintered microstructure [7], and that LPS temperatures for W-Ni-Cu alloys should be between 1400 ^{0}C and 1500 ^{0}C to achieve almost full density [2]. To determine the optimum mixing method to prepare homogeneous W-Ni-Cu alloy powder mixtures, a series of mixing experiments were performed on a selected W-Ni-Cu, namely alloy W-5Ni-5Cu (W5). Four different mixing methods described in section 3.1.3 were applied to this alloy. For each mixing method, 3 samples taken from different parts of the prepared powder mixture batches were compacted at 400 MPa as disc shaped specimens and sintered at 1420^{0}C under pure hydrogen atmosphere for 60 min to achieve fully LPS conditions.

The effects of the mixing methods on the sintering behavior were evaluated on the basis of the variation in the relative density (measured sintered density normalized with respect to theoretical density), composition and microstructure of W5 alloy sintered compacts. The variation of the relative densities (%RD) with different mixing methods is given in Figure 4.1. The matrix compositions of the sintered W5 alloy compacts determined by EDS analysis and their microstructures are presented in Table 4.1 and Figure 4.2, respectively.

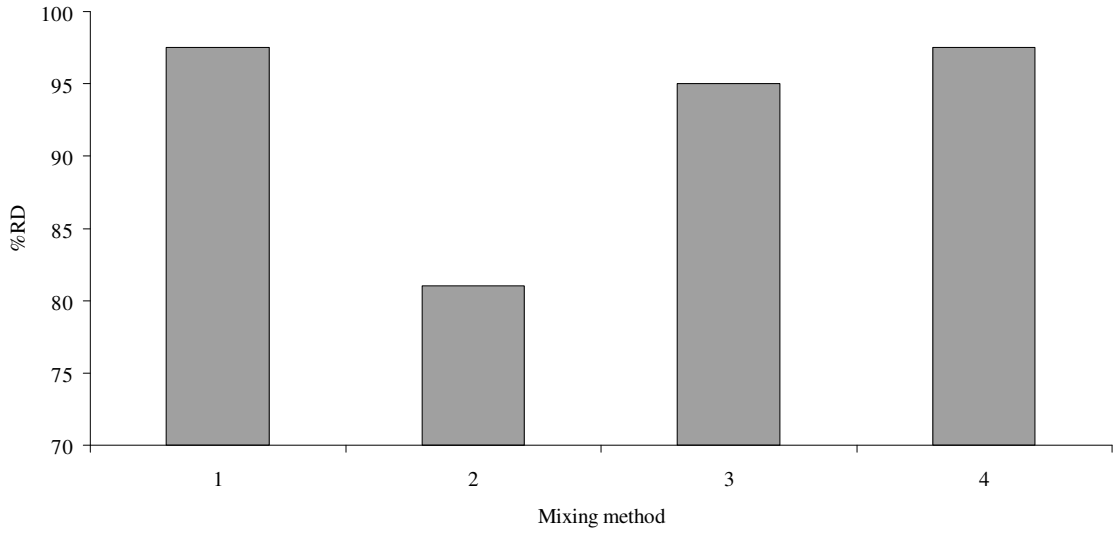

Figure 4.1 The variation in %RD of the sintered compacts with respect to mixing methods; mixing method 1 (without any additive), mixing method 2 (zinc sterate added), mixing method 3 (ethanol added), mixing method 4 (initially Cu-Ni mixed).

Table 4.1 The binder matrix composition of W5 alloy sintered compacts determined by EDS analysis

Mixing Method	Ni (wt%)	Cu (wt%)	W (wt%)
1 (without any additive)	3.79	5.08	91.13
2 (zinc sterate added)	0.19	4.44	95.37
3 (ethanol added)	2.21	2.34	95.45
4 (initially Cu-Ni mixed)	3.32	4.47	92.21

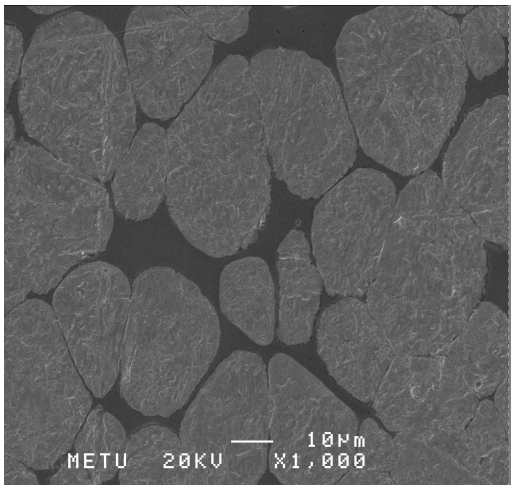

a)

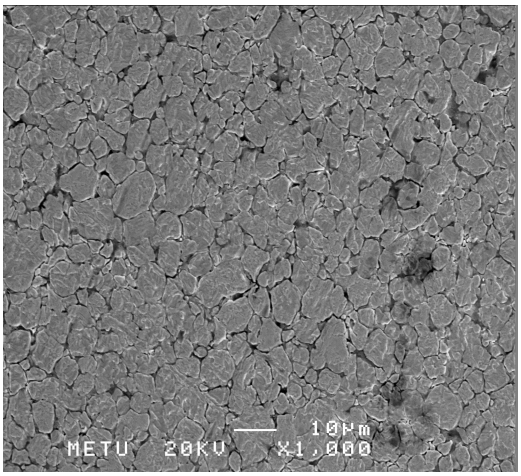

b)

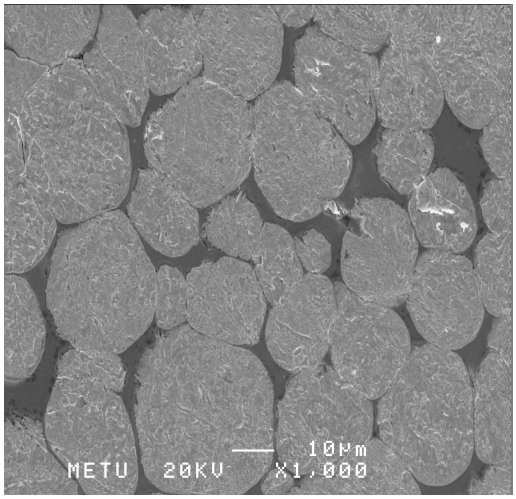

c)

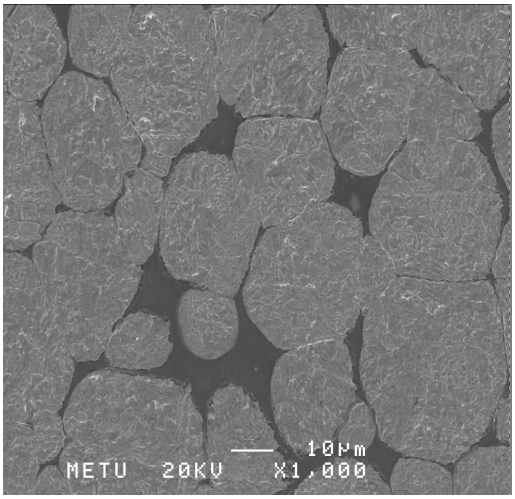

d)

Figure 4.2 SEM Micrographs of W5 alloys a) mixing method (without any additive) 1 b) mixing method 2 (zinc sterate added) c) mixing method 3 (ethanol added) d) mixing method 4 (initially Cu-Ni mixed) X 1,000

Figure 4.1 shows that the nature of the mixing method applied to the W5 alloy samples significantly effects %RD. Samples prepared by mixing methods 1, 3 and 4 showed apparently better densification when compared to samples prepared by stearate addition as lubricant, with slightly lower %RD for mixing method 3, which involved ethanol addition.

As can be seen in Figure 4.2 (a), (c) and (d), W5 alloy samples prepared by mixing methods 1, 3 and 4 showed similar homogeneous microstructures consisting of rounded W particles with completely penetrated binder matrix phase, which is typical of liquid phase sintering. However, the microstructures of the samples prepared by mixing method 2 were found to consist of irregular W particles similar to starting morphology with relatively dark regions dispersed inhomogeneously throughout the microstructure, as can be seen at the right bottom of the micrograph given in Figure 4.2 (b).

Figure 4.2 (b) also implies that there was almost no densification in the sintered compacts prepared by method 2, as also been supported by the %RD results given in Figure 4.1.

EDS analysis results given in Table 4.1 shows that the amount of Ni was relatively lower than the intended amount for all mixing methods. This implies that Ni powder has a stronger tendency to segregate when compared to W and Cu powders. Literature indicates that the blendability is strongly affected by the particle shape [1]. The quality of mixing improves but results in demixing as mixing is continued for the spherical powders. Mixing for one hour may induce demixing of Ni powders, since Ni has almost completely spherical morphology, as can be seen in Figure 3.2

A further examination of the EDS analysis shows that adding zinc stearate to W5 alloy mixtures promoted significant segregation of Ni elemental powder; since only 0.19

wt% elemental Ni could be determined in the EDS analysis of the sintered compact (mixing method 2). It was found in the literature that the addition of zinc stearate added as a surfactant to a powder mixture may cause a change in the flow rates of the elemental powders due to differences in powder size and morphology [1]. The reason of this significant segregation may be attributed to this fact. Moreover, zinc sterate was not completely removed from the compact in the sintering cycle (dark regions observed in Figure 4.2 (b)), this may hinder the diffusion among the constituents resulting in the very poor densification observed.

Both %RD and microstructural examination results suggest that mixing method 3 is as suitable as mixing methods 1 and 4 in preparing homogeneous W-Ni-Cu alloys powder mixtures. However, EDS analysis results clearly show that this method resulted in a significant segregation in W5 alloy powder mixtures, as both Ni and Cu amounts in the sintered compact was found to deviate considerably from the intended amounts. During the preparation of the powder mixtures with mixing method 3, it was experimentally observed that, Cu and Ni elemental powders were brought to the surface of the semi-wet mixture upon ethanol addition. Therefore, this kind of semi-wet condition seems to induce elemental powder segregation during mixing due to the large density differences among W, Ni and Cu elemental powders used in the study.

When the results are evaluated altogether, it can be seen that the nature of the mixing method has a significant effect on the sintering behavior of W-Ni-Cu alloys. As far as the mixing methods investigated in this study are concerned, it can easily be concluded that mixing methods 1 and 4 are the most efficient ones for preparing homogeneous W-Ni-Cu alloys having almost full density. Although these two methods resulted in similar %RD and homogeneous microstructures, mixing time was relatively short in case of mixing method 1. Therefore, this method was selected as the standard mixing method in the preparation of W-Ni-Cu alloys investigated in this study.

4.2 Sintering Studies of W-Ni-Cu Alloys

In this part of the study; the effects of the compaction pressure, W particle size, composition, sintering temperature and time on the sintering behavior of W-Ni-Cu alloys were investigated. Moreover, the model explaining the kinetics of the diffusional processes governing the sintering behavior of W-Ni-Cu alloys was proposed.

4.2.1 Effect of Compaction Pressure and Initial W Particle Size

The effects of compaction pressure and initial W particle size on the sintering behavior of W-Ni-Cu alloys were studied on W-6Ni-4Cu alloy (W6 with W powder having 6μm APS and W6-1 with W powder having 2.5μm APS). W6 and W6-1 alloy powder mixtures mixed by method 1 and compacted into disc shaped specimens with 15 mm diameter and approximately 5 mm height at different pressures as seen in Table 3.3 were sintered at 1420 ^{0}C for 60 min. Since the CIP was used in this study has only a capacity of 414 MPa, the compaction pressures higher than 400 MPa was achieved by using single action hydraulic press. Due to the low compressibility of the spherical elemental powders (Ni and Cu), samples did not acquire enough green strength at compaction pressures lower than 200 MPa for both pressing techniques. Therefore, the minimum compaction pressure was selected as 200 MPa for the compaction studies.

The effect of the compaction pressure and initial W particle size on the sintering behavior of W-Ni-Cu alloys was evaluated on the basis of the variation in %RD of the sintered compacts of W6 and W6-1 alloys. The variation of %RD with compaction pressure and initial W particle size is given in Figure 4.3

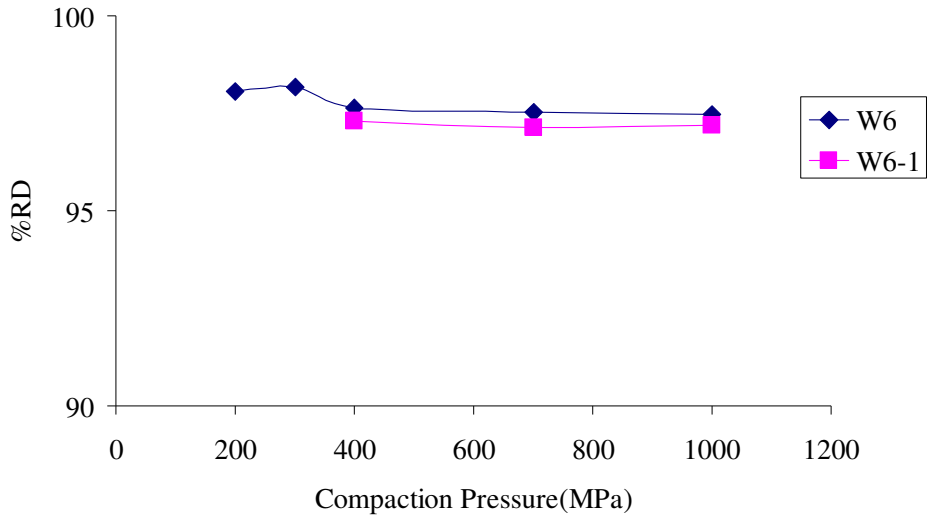

Figure 4.3 The effect of compaction pressure and initial W particle size on %RD for W6 and W6-1 alloys sintered at 1420 ^{0}C for 60 min.

Results given in Figure 4.3 apparently show that there is almost no effect of either compaction pressure or initial W particle size on %RD of sintered W6 and W6-1 alloy compacts, as long as the fully sintered conditions are concerned. It is claimed in the literature that high green density locks the microstructure and inhibits the rearrangement stage of LPS, since an increase in the green density causes much more inter-particle contacts leaving less capillaries important for initial densification. However, if there exist favorable solubility between the constituents and relatively large quantity of liquid, the compaction pressure has little effect on the sintered density [7]. W-Ni-Cu alloys examined in the present study have 10 wt% binder (Ni-Cu) content with differing Ni/Cu ratios and generally show appreciable W solubility in the binder matrix

phase with increasing nickel content, as can easily be realized upon an examination of the ternary W-Ni-Cu phase diagram (see the 1400 ^{0}C isothermal section given in Figure 2.12, for example). Therefore, it is believed that the effect of the compaction pressure on %RD of the sintered compacts was disappeared for W6 and W6-1 alloys, since there exist favorable solubility ratio and adequate amount of liquid in these alloys.

Results given in Figure 4.3 also implies that, densification process for W-Ni-Cu alloys may be dependent mainly on the coarsening stage of liquid phase sintering process, i.e. rearrangement process has almost no effect on densification process for W-Ni-Cu alloys, since compaction pressure has almost no effect on relative densities of the sintered W6 and W6-1 compacts.

According to the above results, a compaction pressure of 400 MPa seems to be optimum for W-Ni-Cu alloys, because there is no need to use higher pressures to achieve higher amount of densification, i.e., %RD

As already mentioned above, initial W particle size does not seem to have any effect on the sintering behaviour of W6 and W6-1 alloys. To investigate whether the initial W particle size has any effect on the final stage coarsening behavior, samples of W6 and W6-1 alloys were cold isostatically compacted at 400 MPa and sintered at 1420 ^{0}C and 1460 ^{0}C under pure hydrogen for 60 min. The results of these experiments were evaluated on the basis of the variations in the average W particle size and %RD of the sintered compacts. The variation in %RD and average W particle size of W6 and W6-1 alloys with respect to the initial W particle size and sintering temperature are given in Table 4.2 and Table 4.3, respectively.

Literature indicates that a small initial particle size improves the densification rate, hence increases the sintered densities for a fixed sintering cycle [7]. In the re-

arrangement stage, a small initial particle size improves the capillary force even though causing increased interparticle friction.

Table 4.2 %RD variation with respect to initial W particle size and sintering temperature

Alloy	Sintering Temperature (^{o}C)	%RD
W6-1	1420	97
W6	1420	97.5
W6-1	1460	97
W6	1460	96.5

Table 4.3 The average W particle Size variation in W6 and W6-1 alloys with respect to the initial W particle size and sintering temperature

Alloy	Sintering Temperature (^{o}C)	Average Particle Size (μm)
W6-1	1420	29.3
W6	1420	29.8
W6-1	1460	33.4
W6	1460	31.9

As can be seen in Tables 4.2 and 4.3, W6 and W6-1 alloys show nearly same values of %RD and average W particle size with respect to sintering temperature. Both %RD and average W particle size examination results suggest that there was no improvement in the densification of W-Ni-Cu alloys with decreasing the APS of W elemental powders from 6 μm to 2.5 μm. As far as W particle sizes investigated in this study are concerned, it can easily be concluded that decreasing initial W particle size has no effect on the densification of W-Ni-Cu alloys. Since smaller initial W particle sizes may cause compaction problems due to stronger interparticle friction, it is advisable to use W powders with an optimum APS in preparing W-Ni-Cu alloys in a feasible way. Based on these results, W powders with 6μm APS were selected as the standard W powder in the preparation of other W-Ni-Cu alloys.

4.2.2 Effect of Composition

The effect of composition on the sintering behavior of W-Ni-Cu alloys are studied on alloys W-1Ni-9Cu (W1), W-2.5Ni-7.5Cu (W2), W-3Ni-7Cu (W3) , W-4Ni-6Cu (W4), W-5Ni-5Cu (W5), W-6Ni-4Cu (W6), W-7Ni-3Cu (W7), W-7.5Ni-2.5Cu (W8). Samples of these alloys were isostatically compacted at 400 MPa and sintered at 1420 ^{0}C under hydrogen for 60 min. The effect of composition was investigated on the basis of the variations in %RD, W solubility in the binder matrix phase, average W particle size, area percentage of the binder matrix phase and microstructure with respect to Ni content in W-Ni-Cu alloys. The variations in %RD, W solubility in the binder matrix phase, average W particle size and area percentage of the binder matrix phase are given in Figures 4.4, 4.5, 4.6 and 4.7, respectively. The microstructures of the sintered compacts are given in Figure 4.8 and Figure 4.9.

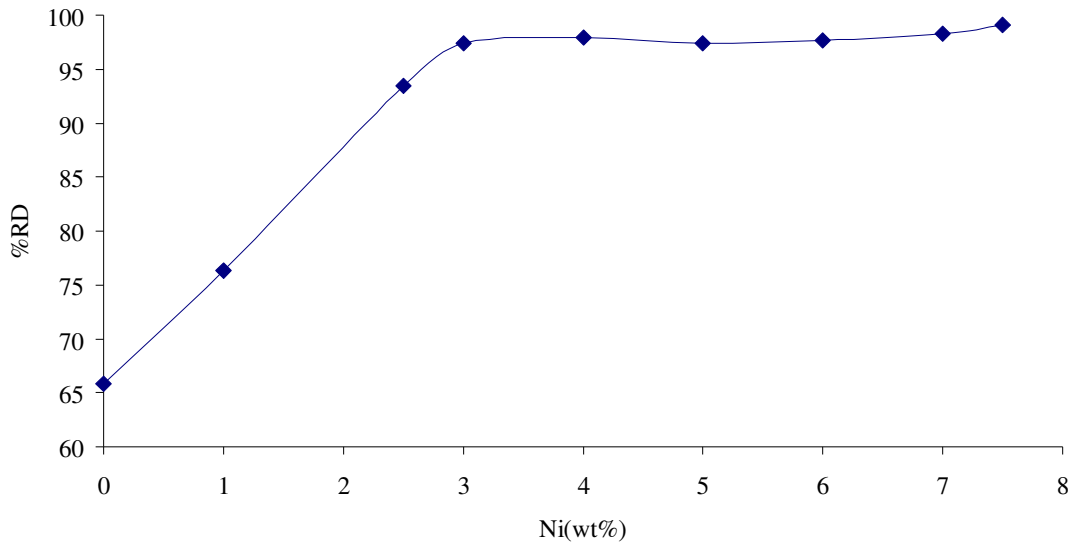

Figure 4.4 The variation in %RD of W-Ni-Cu alloys sintered at 1420 ^{0}C with respect to Ni content

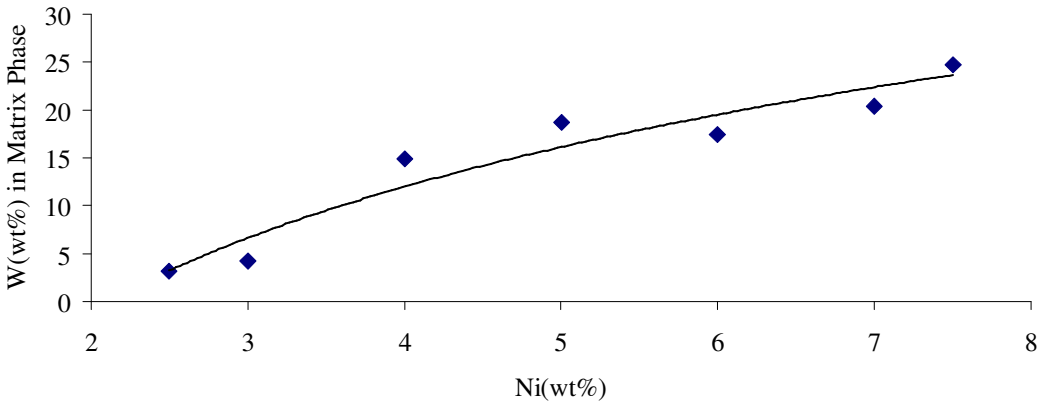

Figure 4.5 The variation in the solubility of W in the binder matrix phase of W-Ni-Cu alloys sintered at 1420 ^{0}C with respect to Ni content determined by EDS analysis.

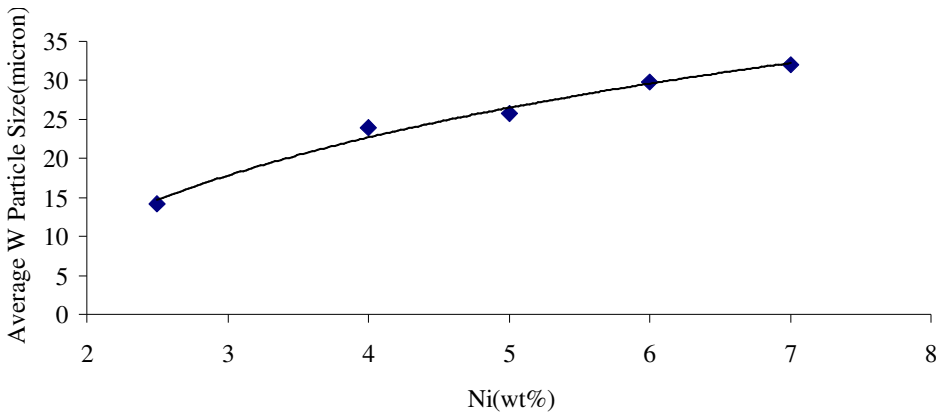

Figure 4.6 Effect of Ni content on average W particle size in W-Ni-Cu alloys sintered at 1420 ^{0}C.

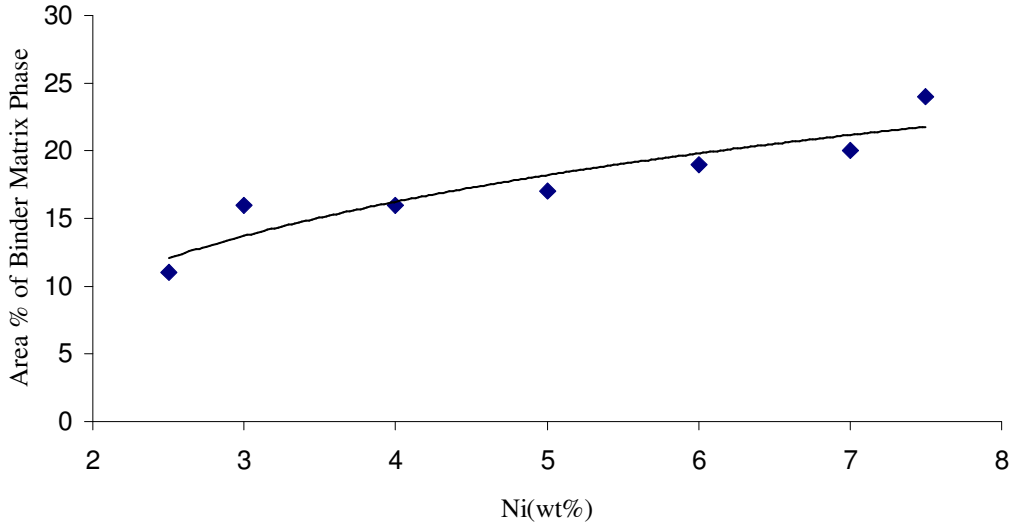

Figure 4.7 Effect of Ni Content on % area of the matrix phase in W-Ni-Cu alloys sintered at 1420 ^{0}C.

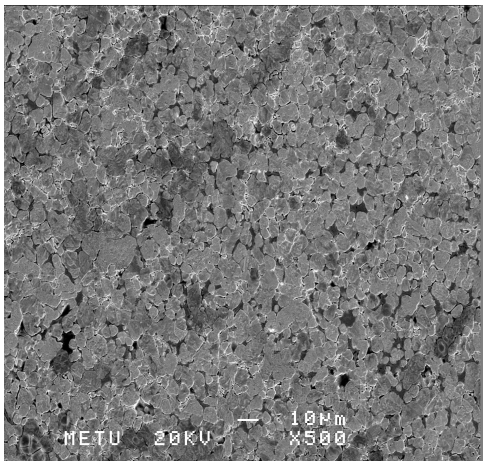

a)

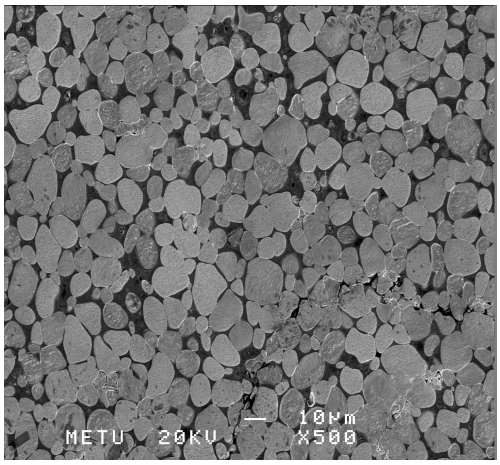

b)

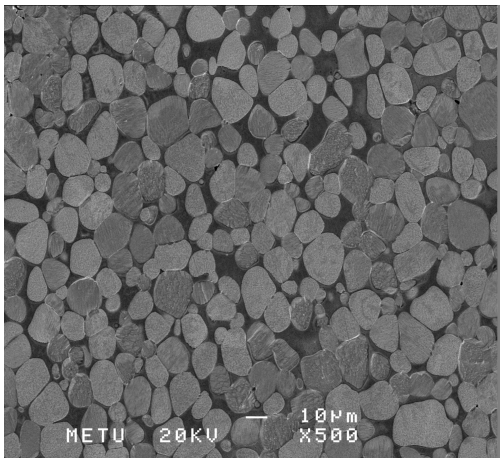

c)

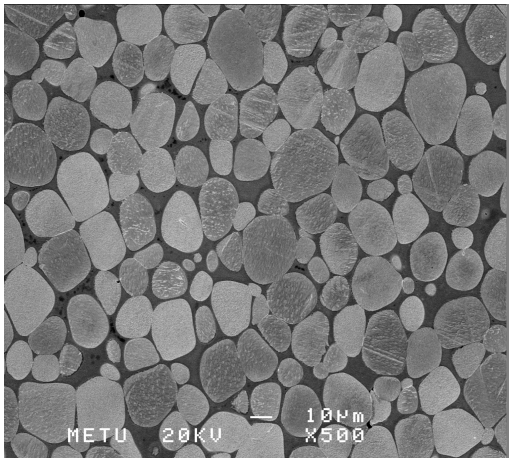

d)

Figure 4.8 Microstructures of W-Ni-Cu alloys sintered at 1420 ^{0}C for 60 min a)W1 b)W2 c)W3 d)W4 X 500

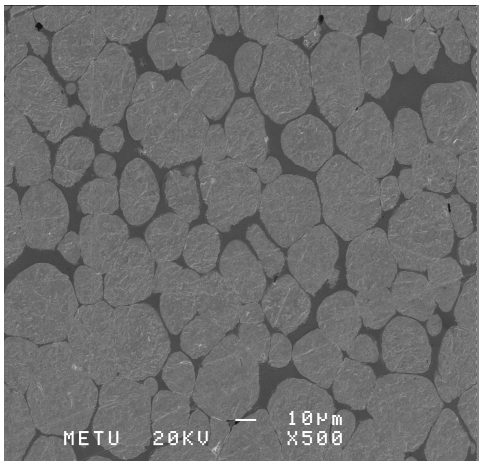

e)

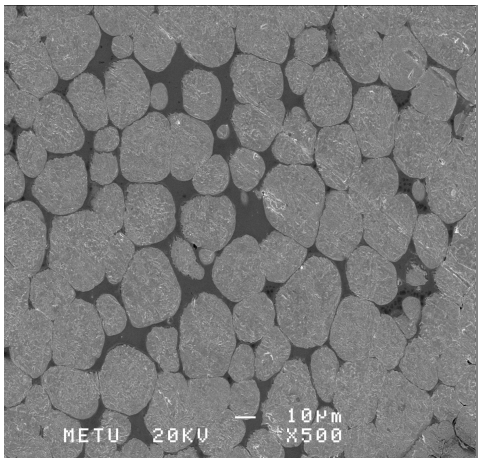

f)

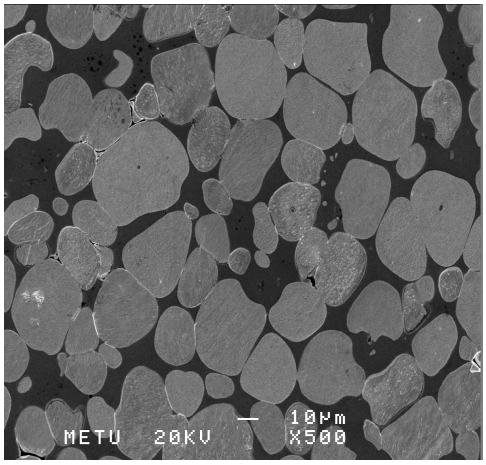

g)

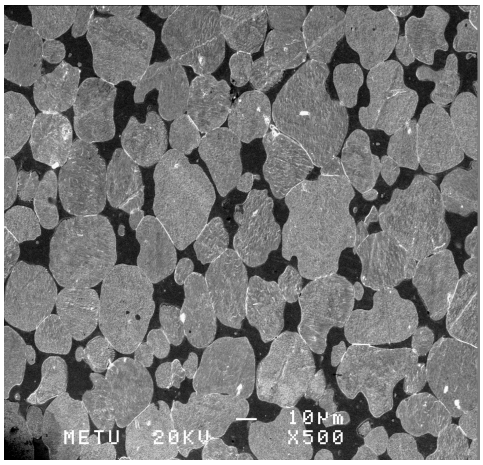

h)

Figure 4.9 Microstructures of W-Ni-Cu alloys sintered at 1420 ^{0}C for 60 min e)W5 f)W6 g)W7 h)W8 X 500

Figure 4.4 shows that %RD of the sintered compacts increases with the Ni content. However, it can be seen that almost full density state is achieved in W-Ni-Cu alloys above about 3 wt% Ni. Figure 4.5, Figure 4.6 and Figure 4.7 reveal that the solubility of W in the binder matrix phase, the average W particle size and the percent area of the binder matrix phase also increase with increase in the Ni content, as also supported by the SEM micrographs of W-Ni-Cu alloys given in Figure 4.8 and Figure 4.9. In these micrographs, the coarsening of W particles and the increase in the percent of the binder matrix phase with increase in Ni content can clearly be observed.

It was cited in the literature that, for complete densification, the system under study should have the following characteristics (a) an appreciable amount of liquid, (b) appreciable solubility of solid-phase particles in liquid and (c) complete wetting of the solid particles by liquid [22]. Therefore, the solubility of W particles in the binder matrix phase is of major concern in the densification of W-Ni-Cu alloys.

Solubility of W in the binder matrix phase strongly depends on the Ni content in W-Ni-Cu alloys, as can be seen in the liquidus projection and 1400 ^{0}C isothermal section of W-Ni-Cu ternary phase diagram, (Fig 2.11 and 2.12). The variation in the solubility of W in the binder matrix phase determined by EDS analysis is given in Figure 4.5. It can easily be realized that the solubility of W in the binder matrix phase increases appreciably with increasing Ni content, as expected. Since W has no solubility in Cu and limited solubility in Ni, overall amount of W particles in a W-Ni-Cu alloy will decrease upon dissolving in the liquid matrix phase. This is the reason why the amount of the binder matrix phase increases in W-Ni-Cu alloys with increase in W solubility, i.e. increase in Ni content, which is seen in Figure 4.7.

When the results are considered altogether, it can be drawn that the sintering behaviour of W-Ni-Cu alloys investigated in this study is essentially dominated by the

Ni content in the alloy, i.e. Ni/Cu ratio. As the Ni content in the alloy increases, the W solubility in the binder matrix phase also increases. While W particles dissolve into the liquid binder matrix phase, the W concentration at the W particle-matrix interface can be assumed to reach its equilibrium value, which can be determined from the equilibrium ternary phase diagram. This means that W concentration at the W particle-matrix interface increases as the Ni content increases in the alloy (See Figure 2.12). As the surface W concentration increases with Ni content, the concentration gradient of W into the binder matrix phase becomes steeper which results in a faster W diffusion. As a result, it is expected that the solubility and subsequent coarsening of W particles occur in a relatively faster rate as Ni content in the alloy increases. This may be the reason why the average W particle size increases with Ni content at the end of the sintering cycle.

4.2.3 Effect of Sintering Temperature

To investigate the effect of the sintering temperature on the densification behaviour of W-Ni-Cu alloys, sintering temperature studies were conducted on W-3Ni-7Cu (W3), W-6Ni-4Cu (W6) and W-7Ni-3Cu (W7) alloys. W3, W6 and W7 alloy samples cold isostatically pressed at 400 MPa were sintered at 1330 ^{0}C, 1375 ^{0}C 1420 ^{0}C under pure hydrogen for 60 min.

The effect of sintering temperature on the sintering behavior was investigated on the basis of the variations in %RD, microstructures, matrix phase microhardness and matrix phase composition of W3, W6 and W7 alloy. The variation in %RD of the sintered compacts of W3, W6 and W7 alloys with respect to temperature are presented in Figure 4.10. The microstructures and binder matrix phase composition and microhardness values of W6 alloy sintered compacts are given in Figure 4.11, Table 4.4 and Figure 4.12, respectively. The trend in the variation of the microstructures, binder

matrix phase composition and microhardness values of W6 are representative for W3 and W7 alloys.

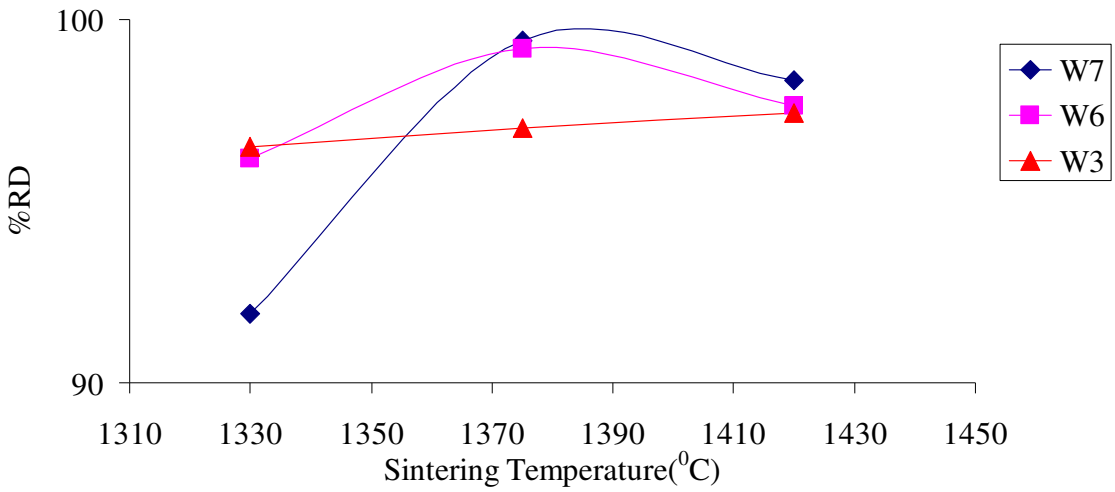

Figure 4.10 Variation in relative densities of sintered compacts of W3, W6, W7 alloys with respect to sintering temperature

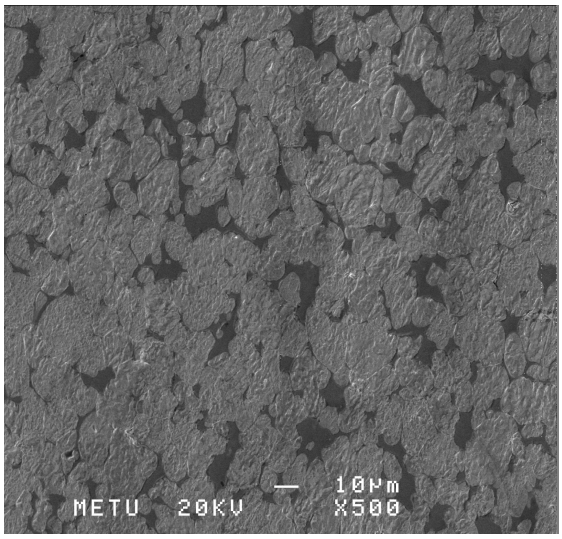

a)

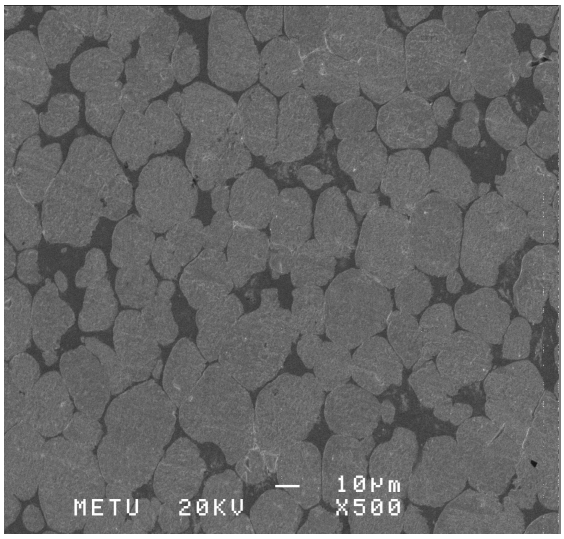

b)

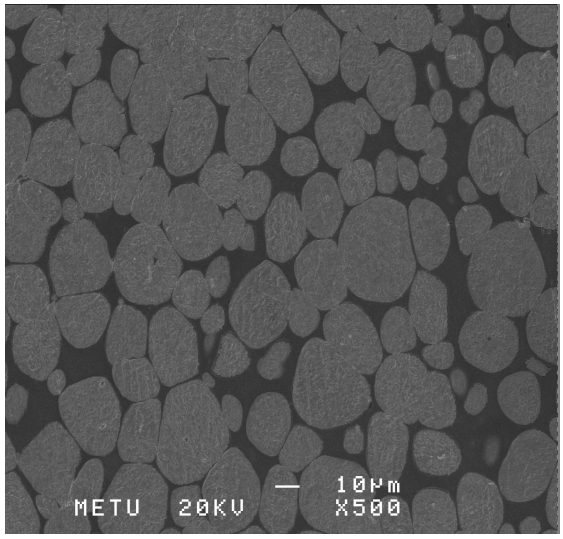

c)

Figure 4.11 SEM micrographs W6 alloy compacts sintered for 60 min at a) 1330 ^{0}C b) 1375 ^{0}C c) 1420 ^{0}C X 500

Table 4.4 EDS spot analysis of binder matrix phase of W6 alloys sintered at 1330 ^{o}C, 1375 ^{o}C, 1420 ^{o}C.

Alloy	Sintering Temperature (^{o}C)	Ni (wt%)	Cu (wt%)	W (wt%)
W6	1330	56.03	27.88	16.08
W6	1375	53.55	27.58	18.87
W6	1420	58.84	23.19	17.97

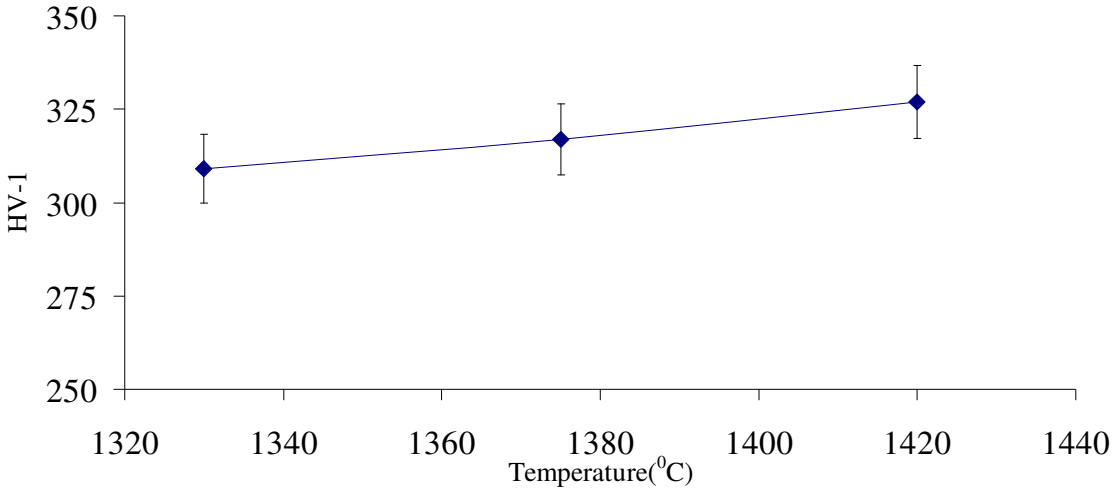

Figure 4.12 Variation in hardness of W6 alloys with respect to sintering temperature

Results given in Figure 4.10 show that densification of W-Ni-Cu alloys strongly depend on sintering temperature. While %RD of W3 increases monotonically with the sintering temperature, %RD of W6 and W7 alloys first increase then decrease with sintering temperature. At low temperatures, W3 and W6 alloy samples have relatively higher %RD, but with increase in temperature W7 alloy samples have relatively higher %RD.

Figure 4.11 provides comprehensive comparison of the microstructures of W6 alloy sintered compacts as sintering temperature increases from 1330 ^{0}C to 1420 ^{0}C. For W6 alloy, at 1330 ^{0}C, W particles are small and irregular and it was found that some W particles were not completely penetrated by the liquid matrix phase, as can be seen in Figure 4.14. At 1375 ^{0}C and 1420 ^{0}C the microstructure shows relatively more rounded W particles with a completely penetrating matrix phase typical of liquid phase sintering.

Figure 4.12 reveals that the microhardness of the sintered W6 samples increases with increase in sintering temperature.

The results can be discussed as follows:

As sintering temperature increases, the densification in terms of %RD increases appreciably due to the formation of a liquid phase which greatly aids the densification (see Figure 4.10). Therefore, the melting range of the binder matrix phase becomes very important for the densification process. In the case of liquid phase sintering for W-Ni-Cu alloys, after melting of copper at about 1081^{0}C, it believed that there occurs very fast diffusional alloying between Cu and Ni. Before complete Ni dissolution in the resulting liquid, interactions between W and Ni can be ignored. Therefore solidus and liquidus temperatures of the binder matrix phase can be determined roughly by the help of Cu-Ni binary phase diagram given in Figure 3.3. W3, W6 and W7 alloys have different solidus

temperatures for the Ni-Cu binder matrix phase, which are determined as 1200 ^{0}C, 1315 ^{0}C, 1350 ^{0}C, respectively, from the phase diagram. Due to its low solidus temperature, the formation of the liquid phase begins at lower temperatures for W3 alloy. This implies that densification of W3 alloy may start at lower temperatures when compared to other alloys.

In liquid phase sintering process, significant densification can be achieved if there exist adequate amount of liquid binder matrix phase and appreciable W solubility in the matrix. However, the amount of W solubility in the matrix phase can not be solely determined by using Cu-Ni binary phase diagram. Assuming that equilibrium is reached at any sintering temperature, the isothermal section of the ternary W-Ni-Cu phase diagram at the relevant sintering temperature can be used to determine the amount of the phases present and their solubilities among each other. To aid in discussion, the 1300 ^{o}C and 1400 ^{o}C isothermal sections of W-Ni-Cu ternary phase diagram are given in Figure 4.13. As can be inferred through interpolation from this figure, in the case of sintering at 1330 ^{0}C, W7 alloy falls in either W (solid)+L (W+Ni+Cu)+S (W+Ni+Cu) or W (solid)+S (W+Ni+Cu) phase regions. This implies that, the binder phase in W7 alloy is either completely solid or consists of a liquid-solid mixture at that sintering temperature. It is thought that at 1330 ^{0}C, diffusion rate or mass transport rate during sintering from W particle to Ni-Cu matrix should be determined by the degree to which the binder matrix phase become liquid, since for any diffusion process, the diffusivity in the liquid is much higher than that in the solid. Since the amount of liquid in W7 alloy seems to be lower at 1330 ^{0}C, its %RD remained low at this temperature. On the other hand, at temperatures 1375 ^{0}C, and 1420 ^{0}C, W7 alloy has an appreciable amount of liquid binder matrix phase and hence reaches to almost full density. Diffusion rate is determined by the Ni amount of the alloy if the sintering temperature is same for W3 and W6 alloys. The concentration gradient of W in the liquid phase at the particle matrix surface increases with increase in Ni amount which dictates the solubility of W in binder

matrix. As illustrated in Table 4.4, with increasing sintering temperature from 1330 ^{0}C to 1420 ^{0}C, solubility of W in Cu-Ni liquid matrix for W6 alloy increases. This shows that liquid that occurred as sintering temperature increases has enough solubility for W particles to penetrate the W particles which resulted in concentration gradient from W particles to binder matrix phase. This favors the high diffusion rate between between liquid binder matrix phase and W particles. High diffusion rate induces the high densification by increasing overall kinetics of re-arrangement and coarsening stages of liquid phase sintering in W-Ni-Cu alloys. This increase in W solubility in binder matrix results in high densification resulting in the microstructure consisting of rounded and coarsened W particles as can be seen in Figure 4.11 (c). The dissolved W in the binder matrix provides more hardness as sintering temperature increases as can be seen in Figure 4.12 since microhardness of the W6 alloy sintered compacts was dominated by the W solubility in binder matrix phase.

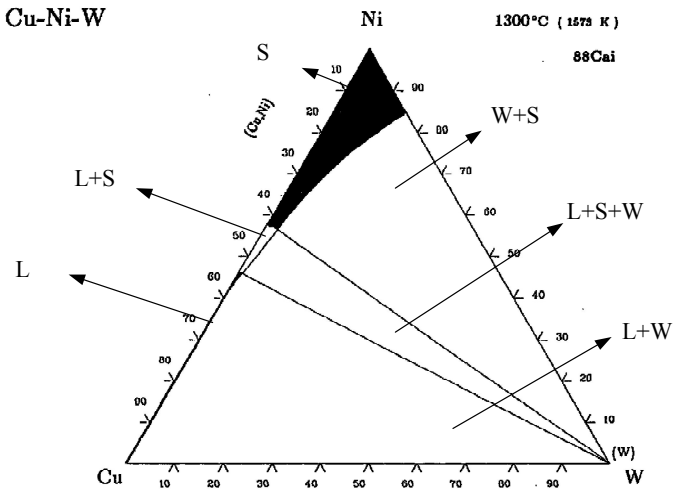

a)

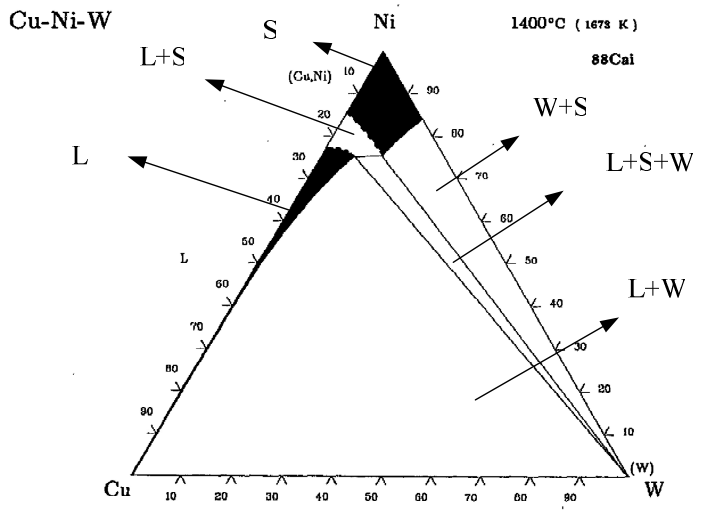

b)

Figure 4.13 Isothermal section of W-Ni-Cu alloy at a)1300 ^{o}C b) 1400 ^{o}C [19].

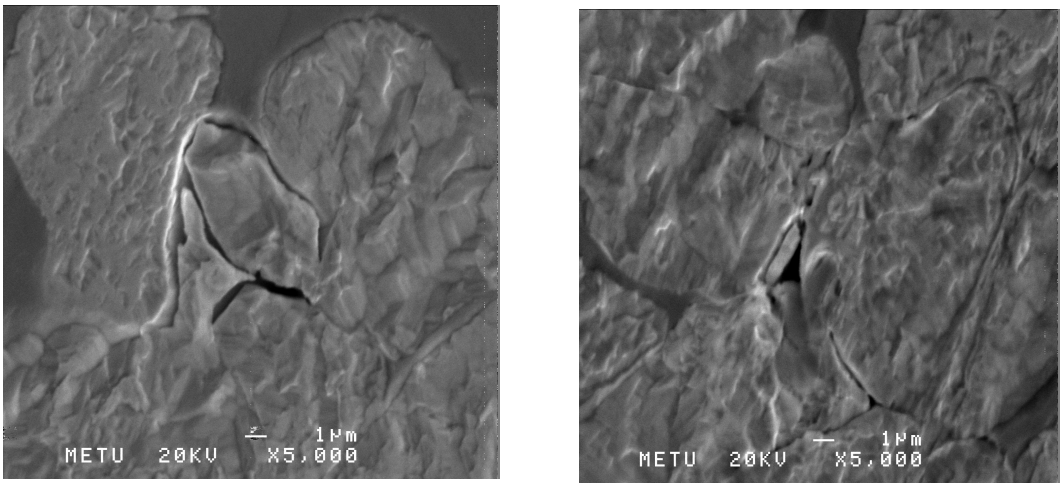

Figure 4.14 SEM micrographs of Irregular W particles which were not penetrated by liquid binder matrix phase of W6 alloy sintered at 1330 ^{0}C for 60 min X 5,000

4.2.4 Effect of Sintering Time

To determine the effect of the sintering time on the sintering behaviour for W-3Ni-7Cu (W3), W-6Ni-4Cu (W6) and W-7Ni-3Cu (W7) alloys, mixtures cold isostatically compacted at 400 MPa were sintered at 1420 ^{0}C for 15, 30 and 60 min, respectively. The investigation of the effect of sintering time on densification of W-Ni-Cu alloys will be based on the change in %RD, average W particle size and microstructures of the sintered compacts with respect to sintering time.

The variation in the %RD of W3, W6 and W7 alloys and the variation in the average particle size of W6 and W7 alloys with respect to sintering time are given in

Figures 4.15 and 4.16, respectively. Furthermore, optical micrographs of W3, W6 and W7 alloys are given in Figures 4.17, 4.18 and 4.19, respectively.

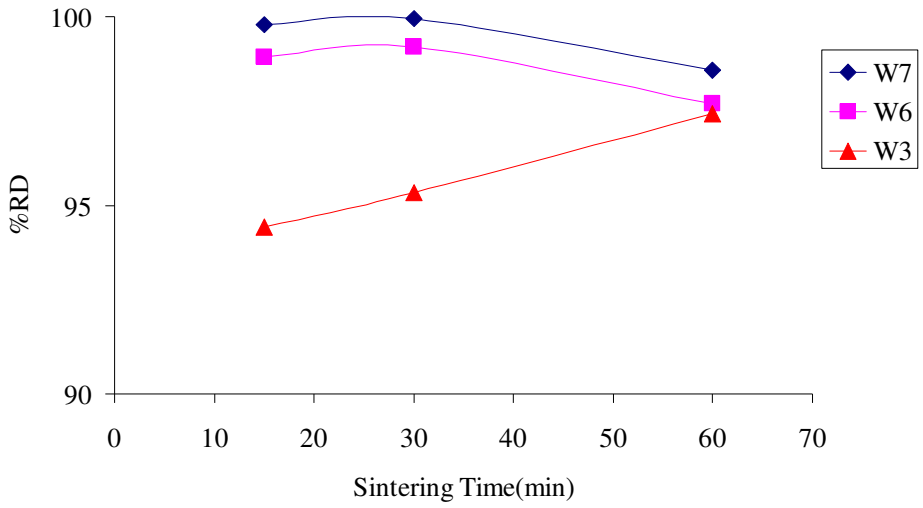

Figure 4.15 Variation in relative densities of W7, W6 and W3 alloys sintered at 1420 ^{0}C with respect to sintering time.

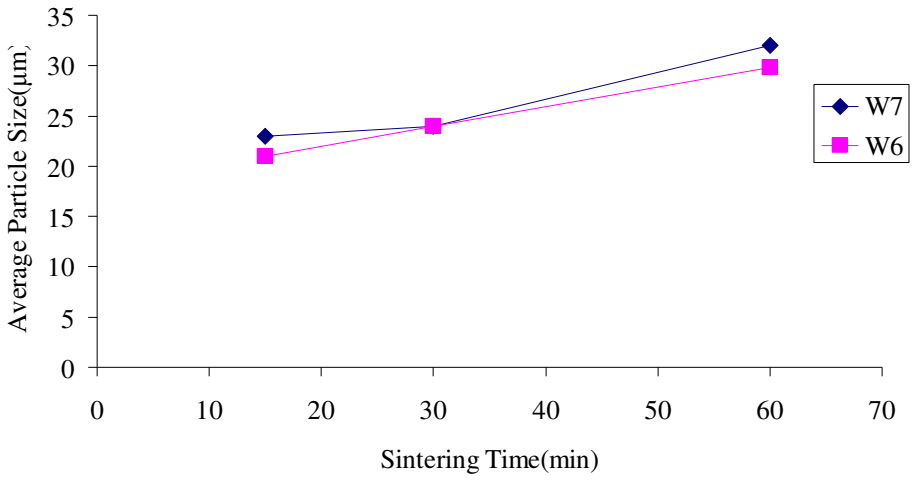

Figure 4.16 Change in average particle size of W6 and W7 alloys with respect to sintering time.

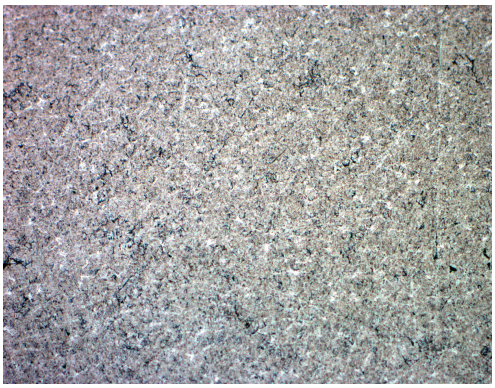

a)

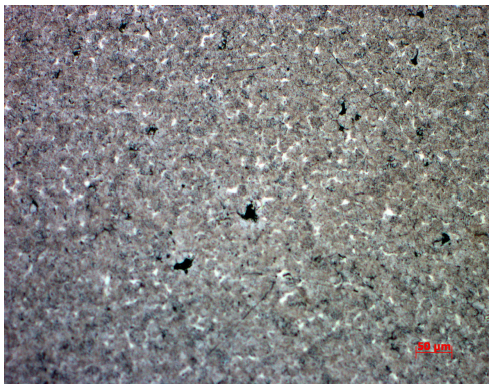

b)

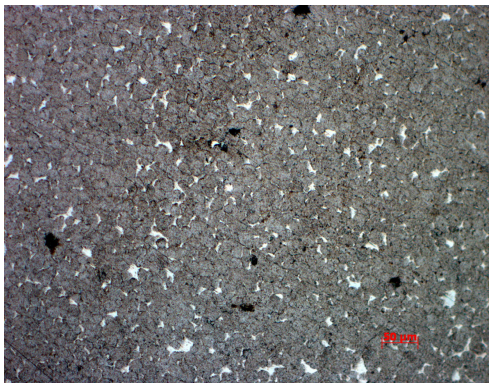

c)

Figure 4.17 Optical Micrographs of W3 alloys sintered at 1420 ^{0}C a) 15min b) 30 min c) 60min X 200

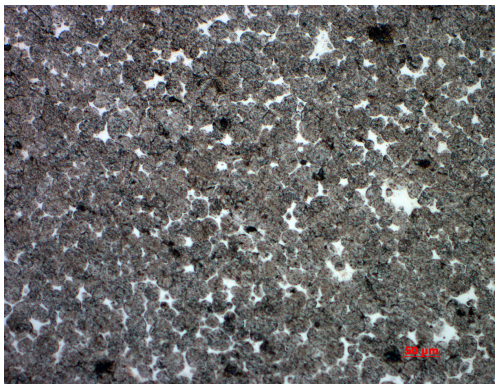

a)

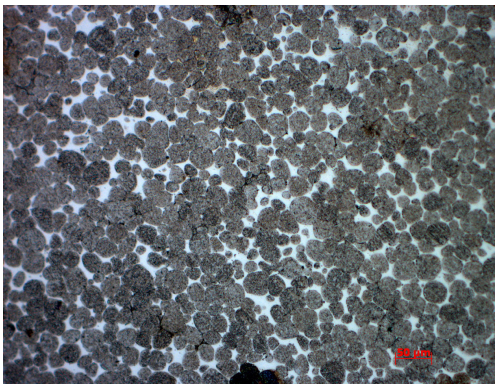

b)

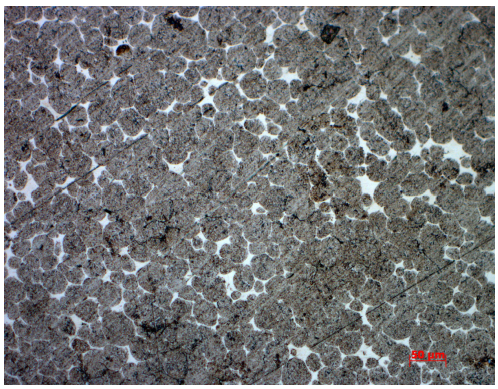

c)

Figure 4.18 Optical Micrographs of W6 alloys sintered at 1420 ^{0}C a) 15min b) 30 min c) 60min X 200

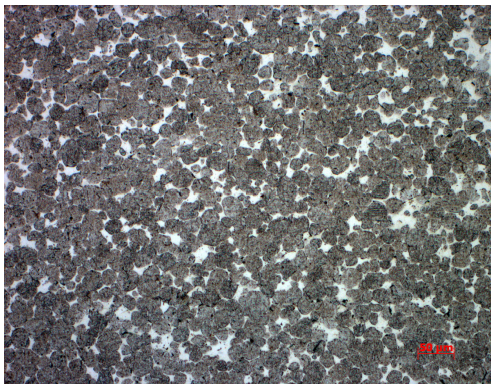

a)

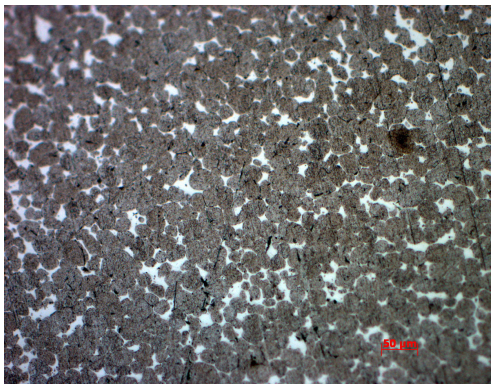

b)

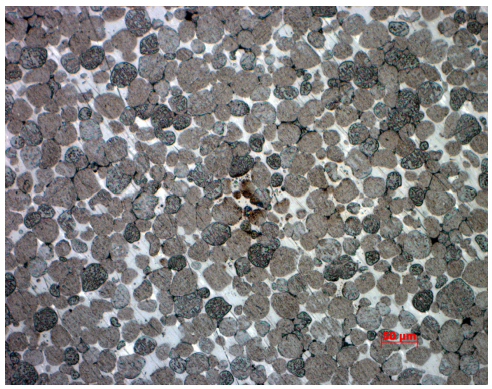

c)

Figure 4.19 Optical Micrographs of W7 alloys sintered at 1420 ^{0}C a) 15min b) 30 min c) 60min X 200

As can be seen in Figure 4.15, W6 and W7 alloy samples showed the same trend in %RD of the sintered compacts with respect to sintering time. In other words, there was a slight decrease that can be neglected in relative density of W6 and W7 alloys as sintering time passes, however %RD of W3 alloy sintered compacts increases as sintering time passes. The results given in Figure 4.16 indicates that average particle size of W6 and W7 alloy increases with increase in sintering time; i.e. W particle coarsens as sintering time passes. It should be also remarked that W7 coarsened more than W6 alloys at the same sintering time. Figure 4.16 does not include the variation of average W particle size of W3 alloy with sintering time, since average particle size of W3 alloy could not be clearly determined. Results given in Figure 4.16 are supported by the optical micrographs of W3, W6 and W7 alloys. It is easily observed that W particles showed significant coarsening as can easily be seen in Figures 4.18(c) and 4.19(c), however, W particle coarsening behavior could not be clearly observed in W3 alloy as shown in Figure 4.17, since pore elimination was not completed up to 60 min in W3 alloy.

When all the results are considered together, it was concluded that sintering time between 15 and 30 min was enough to achieve almost full density with a small average W particle size for W7 and W6 alloys. However, as time passes although there was no increase in %RD of the W6 and W7 alloys, average W particle size increases appreciably, which resulted from the strong dependency of solubility of W particles on the curvature of the W particle. Concentration at surface of W particles is increased above the equilibrium value because of the surface curvature. This concentration gradient induces the diffusion from small particles to large particles. Therefore, large W particles grow at the expense of small particles reduce the surface potential. However, this phenomenon can not be observed in W3 alloy, since densification did not complete at these time intervals. W3 alloys required much more time to achieve same amount of densification in terms of %RD and to start to coarsen.

Rate of atom loss from W particle, i.e. coarsening rate, is controlled by diffusion coefficient in the liquid matrix and radial concentration gradient of W particles in the Ni-Cu matrix at the W particle-matrix surface. Kothari et al [22] showed that, diffusion in matrix increases with the Ni content at constant sintering temperature and for the same binder amount. Therefore, W7 alloy has higher average particle size than W6 alloy and W3 alloy requires relatively long time to coarsen and achieve same %RD, since coarsening and densification was reduced by low solubility of the W atoms in the matrix.

4.2.5 Diffusional Model Studies on W-Ni-Cu Alloys

The results of the study have shown that the sintering behavior of W-Ni-Cu alloys investigated in this study was essentially dominated by the Ni content in the alloy and the sintering temperature. It was also found that the W solubility in the binder matrix phase was directly proportional to these variables, i.e. it increased with increasing Ni content and sintering temperature. Moreover, the degree of coarsening of W particles was also found to be directly proportional to these variables and also sintering time. All of these experimental evidences imply that sintering behavior of W-Ni-Cu alloys is mainly governed by diffusional processes. Therefore, a model was proposed to explain the sintering kinetics in these alloys in terms of the diffusional processes taking place in the initial dissolution and final coarsening stages. As an aid to the following discussion, 1400 ^{0}C isothermal section of W-Ni-Cu ternary alloy system is given in Figure 4.20. Since the compositions are given in atomic percentages in this figure, the compositions of the alloys to be considered will also be given in atomic percentages throughout the following discussion.

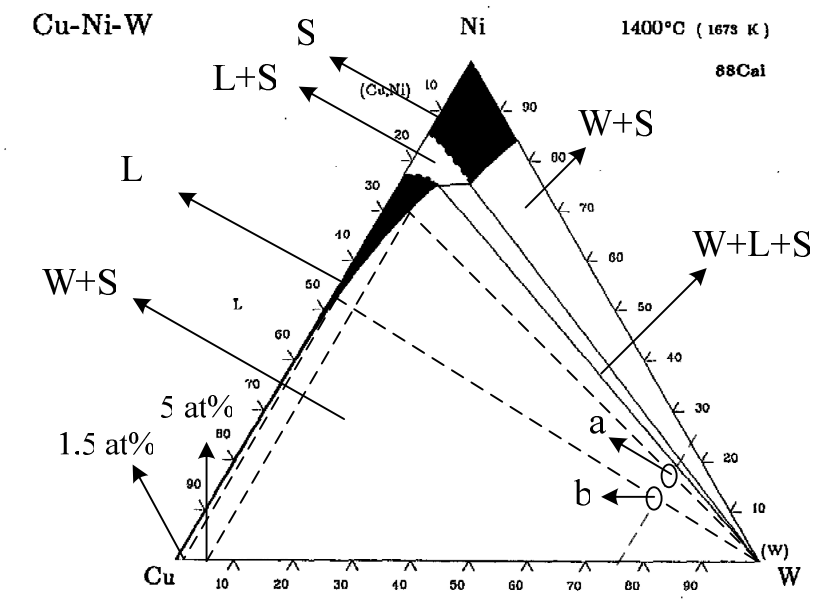

Figure 4.20 1400 ^{0}C isothermal section of W-Ni-Cu ternary alloys. a:W-17Ni-8Cu, b:W-13Ni-12Cu

In practice, W-Ni-Cu alloys are mainly produced by using LPS method, which was also the case in this study. Therefore, only the case in which the binder matrix phase is fully liquid will be considered below.

For this case, the sintering temperature is chosen to be 1400 ^{0}C. Two W-Ni-Cu alloys having different Ni content are chosen for the discussion; namely a: W-17Ni-8Cu, b:W-13Ni-12Cu, both in atomic percentages. The samples of these alloys are assumed to be brought to the sintering temperature immediately. It is known form the binary phase diagram data that Cu and W has almost no mutual solubility to each other, W can dissolve in Ni appreciably, there is a complete solubility between Cu and Ni and Ni has

almost no solubility in W at this temperature. For both of the alloys, the sintering process is expected to begin and continue as follows;

At the very beginning, W, Ni, and Cu powders are pure individual particles. When the sintering temperature reaches to 1400 ^{0}C immediately, Cu powders becomes fully liquid in a very short time due to its melting point about 1081^{0}C. After Cu melts in the powder mixture, very fast diffusional alloying is expected to take place between Ni and Cu. Therefore, interactions between solid W and solid Ni can be ignored at that stage. Amount of the solid Ni decreases rapidly since Cu, which is completely liquid, dissolves Ni rapidly. After a certain amount of time, completely liquid Ni-Cu binder matrix phase is achieved. Although W has no solubility in Cu, liquid Ni-Cu matrix phase is able to dissolve W. Solubility of W in Ni-Cu liquid can be determined from the values marked Figure 4.20, which are 1.5 at% W for “alloy b” and 5 at% W for “alloy a”. Assuming the local equilibrium exists at the interface between the binder matrix phase and W particles, W concentration at this interface can be taken as 1.5 at% W for “alloy b” and 5 at% W for “alloy a”. Hypothetical diffusion couples representing this situation are given in Figure 4.21;

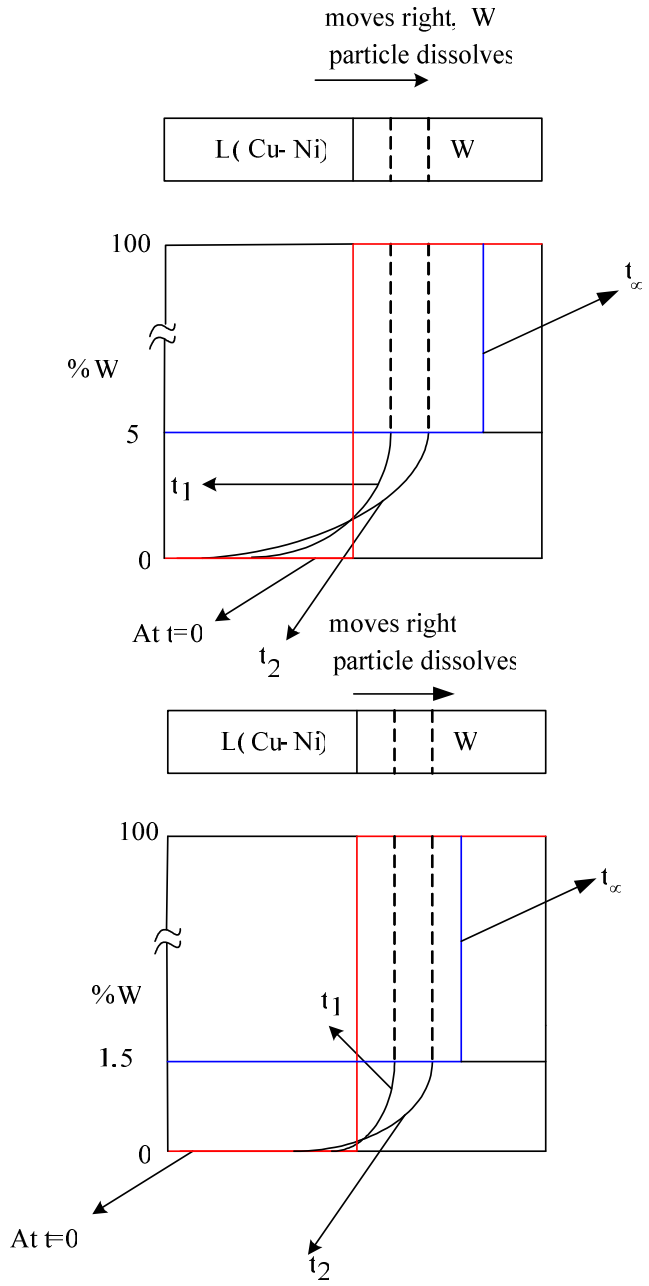

Figure 4.21 Diffusion couples representing the dissolution stage of the W particles ($t_1<t_2$)

As can be seen in Figure 4.20, the W concentration gradient is much higher at the interface between the binder matrix phase and W particles for “alloy a”. Therefore dissolution is faster and higher for the “alloy a” as compared to the “alloy b”. As a consequence, W dissolution stage finishes in a shorter time and this alloy begins to coarsen in a shorter time than the “alloy b”. At this stage, i.e. during dissolution of W particles in the liquid matrix, kinetics is expected to obey the square root law ($X=k\sqrt{t}$) as in any simple diffusional phenomena. The shrinkage of the W particles and increase in the liquid phase amount can be calculated by level rule application. Once the liquid matrix is saturated wit equilibrium amount of W, coarsening due to surface curvature dependent solubility commences. This phenomenon also known as Oswald ripening, is well documented [25,26,27] and because of its statistical nature obey $t^{1/3}$ kinetics. Average particle radius will increase as the one third powder of time and one third power of the equilibrium concentration of the W particle, therefore “alloy a” coarsens more than “alloy b” in a given time due to its higher equilibrium W concentration.

As a result, the following can be concluded: as the Ni content in W-Ni-Cu alloys increases, the equilibrium solubility of W in the alloy also increases, this results in a higher W concentration gradient in the binder matrix phase which results in faster dissolution of W particles. Moreover, the high equilibrium W concentration also increases the coarsening rate. Therefore, Ni rich W-Ni-Cu alloys show faster overall kinetics.

CHAPTER 5

CONCLUSION

In the present study concerning the production of W-Ni-Cu alloys from elemental powders by conventional mixing, cold compaction and sintering, the following major conclusions have been drawn:

1- The nature of the mixing method has a significant effect on the sintering behavior of W-Ni-Cu alloys. Appropriate mixing technique determined as the one without use of any additives, should be used to achieve the homogeneous microstructure and almost full density in W-Ni-Cu alloys.

2- As long as the fully sintered conditions are concerned, compaction pressure and initial W particle size has almost no effect on the sintering behaviour of W-Ni-Cu alloys.

3- The sintering behaviour of W-Ni-Cu alloys investigated in this study is essentially dominated by the Ni content in the alloy, i.e. Ni/Cu ratio. Almost full density can only be achieved in W-Ni-Cu alloys with Ni/Cu ratio greater than 3/7. This is attributed to the increase in W solubility in the binder matrix phase which resulted in increase in the concentration gradient of W into the binder matrix phase, hence diffusion.

4- Densification and coarsening rate of W particles in W-Ni-Cu alloys increase appreciably with sintering temperature due to the increase in the amount of the binder matrix phase and diffusivity of W atoms.

5- Based on the results obtained in the present study, a model explaining the kinetics of the diffusional processes taking place in the sintering (densification) stage was proposed.

REFERENCES

[1] Metals Handbook, Ninth Edition, Volume 7, American Society for Metals, Ohio, 1989.

[2] K. Chattopadhyay, Microstructural characterization of sintered W-Ni-Cu alloys, M.S. Thesis, Indian Institute of Technology, April 2003.

[3] Randall M. German, Powder Metallurgy Science, Metal Powder Industries Federation, Princeton, New Jersey, 1984.

[4] Z. Esen, Master Thesis in Met.& Mat. Engineering, METU, Ankara, TURKEY, 2002.

[5] P. J. James, Powder Metal. Int., 1982, 4, pp.82

[6] Qintus Isostatic Pressing Handbook, April 1984

[7] R.M. German, Sintering Theory and Practice, John Wiley and Sons, Inc., New York, 1996.

[8] S. -J. L. Kang, Sintering, Densification, Grain Growth, and Microstructure, Elsevier Butterworth-Heinemann, 2005

[9] H. S. Cannon and F. V. Lenel, Some observations on the mechanism of liquid phase sintering, in Pulvermetallurgie (Plansee Proceedings 1952), F. Benesovsky(ed.), Metallwerk Plansee GmbH, Reutte, 106-22, 1953.

[10] W. D. Kingery, Densification during sintering in the presence of a liquid phase. I.Theory, J.Appl. Phys., 30, 301-306, 1959.

[11] O. J. Kwon and D. N. Yoon, The liquid phase sintering of W-Ni, in sintering processes (Proc. 5th Inter. Conf. on Sintering and Related Phenomena), G. C. Kuczynski (ed.), Plenum Press, New York, 208-18, 1980.

[12] S. -J. L. Kang, K-H. Kim and D.N. Yoon, Densification and shrinkage during liquid phase sintering, J.Am. Ceram. Soc., 74,425-27, 1991.

[13] S. -M. Lee and S. -J. L. Kang, Theoretical analysis of liquid sintering: pore filling theory, Acta Mater., 46, 3191-202, 1998.

[14] R. M. German, S. Farooq and C. M. Kipphut, Kinetics of liquid phase sintering, Materials Science and Engineering, A 105/106 215-224, 1988

[15] H. -H. Park, O. –J Kwon and D. N. Yoon, The critical grain size for liquid flow into pores during liquid phase sintering, Metall. Trans. A, 17A, 1915-19, 1986.

[16] N. C. Kothari, Sintering kinetics in tungsten powder, Journal of the Less Common Metals, 5, 140-150, 1963.

[17] I. H. Moon, J. H. Kim, M. J. Suk, K. M. Lee and J. K. Lee, Observation of W particle growth in a W powder compact during sintering in a non-reducing atmosphere, Refractory Metals& Hard Materials, 11, 309-315, 1992.

[18] G. H. S. Price, C. J. Smithels, and S. V. Williams, "Sintered alloys. Part I.-Copper-Nickel-Tungsten alloys sintered with a liquid phase present," Journal of Institute. Metals, vol 62(1938) pp.239.

[19] Handbook of ternary alloy phase diagrams, ASM international, 1995.

[20] K. N. Ramakrishnan, G. S. Upadhyaya, Effect of composition and sintering on the densification ad microstructure of tungsten heavy alloys containing copper and nickel, Journal of Materials Science Letters, 9, 456-459, 1990.

[21] V. Srikanth and G. S. Upadhyaya, Effect of tungsten particle size on sintered properties of heavy Alloys, Powder Technology, 39, 61-67, 1984

[22] N. C. Kothari, Densification and grain growth during liquid phase sintering of tungsten-nickel-copper alloys, J.less common metal, 13, 457-468, 1967

[23] R. Makarov, O. K. Teodorovich and I. N. Fruntsevich, The coalescence phenomena in liquid phase sintering in the systems W-Ni-Fe and W-Ni-Cu, Soviet Powder Metallurgy and Metal ceramic, vol.4, 1965, pp.554-559.

[24] Y. Wu, R. M. German , B. Marx, R .Bollina, M. Bell, Characteristics of densification and distortion of Ni_ Cu liquid-phase sintered tungsten heavy alloy, Materials Science and Engineering A344 (2003) 158_ 167

[25] J. M. Lifshiftz and V. V. Slyozov, J.Phys. Chem. Solids 19, 35, 1961.

[26] C. Wagner, Z. Elektrochem. 65, 581, 1961.

[27] J. C. Cahn, in The mechanism of phase transformations in crystalline solids, Institute of Metals Monograph No.33, Institute of Metals, London, 1961.